ULTRAFAST LASERS

Technology and Applications

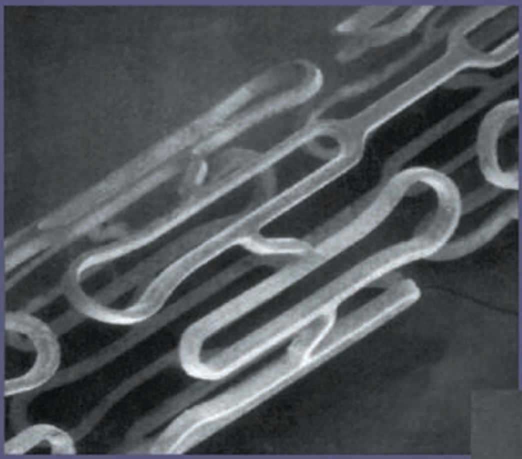

edited by

Martin E. Fermann

Almantas Galvanauskas

Gregg Sucha

ULTRAFAST LASERS

OPTICAL ENGINEERING

1. Electron and Ion Microscopy and Microanalysis: Principles and Applications, *Lawrence E. Murr*
2. Acousto-Optic Signal Processing: Theory and Implementation, *edited by Norman J. Berg and John N. Lee*
3. Electro-Optic and Acousto-Optic Scanning and Deflection, *Milton Gottlieb, Clive L. M. Ireland, and John Martin Ley*
4. Single-Mode Fiber Optics: Principles and Applications, *Luc B. Jeunhomme*
5. Pulse Code Formats for Fiber Optical Data Communication: Basic Principles and Applications, *David J. Morris*
6. Optical Materials: An Introduction to Selection and Application, *Solomon Musikant*
7. Infrared Methods for Gaseous Measurements: Theory and Practice, *edited by Joda Wormhoudt*
8. Laser Beam Scanning: Opto-Mechanical Devices, Systems, and Data Storage Optics, *edited by Gerald F. Marshall*
9. Opto-Mechanical Systems Design, *Paul R. Yoder, Jr.*
10. Optical Fiber Splices and Connectors: Theory and Methods, *Calvin M. Miller with Stephen C. Mettler and Ian A. White*
11. Laser Spectroscopy and Its Applications, *edited by Leon J. Radziemski, Richard W. Solarz, and Jeffrey A. Paisner*
12. Infrared Optoelectronics: Devices and Applications, *William Nunley and J. Scott Bechtel*
13. Integrated Optical Circuits and Components: Design and Applications, *edited by Lynn D. Hutcheson*
14. Handbook of Molecular Lasers, *edited by Peter K. Cheo*
15. Handbook of Optical Fibers and Cables, *Hiroshi Murata*
16. Acousto-Optics, *Adrian Korpel*
17. Procedures in Applied Optics, *John Strong*
18. Handbook of Solid-State Lasers, *edited by Peter K. Cheo*
19. Optical Computing: Digital and Symbolic, *edited by Raymond Arrathoon*
20. Laser Applications in Physical Chemistry, *edited by D. K. Evans*
21. Laser-Induced Plasmas and Applications, *edited by Leon J. Radziemski and David A. Cremers*
22. Infrared Technology Fundamentals, *Irving J. Spiro and Monroe Schlessinger*
23. Single-Mode Fiber Optics: Principles and Applications, Second Edition, Revised and Expanded, *Luc B. Jeunhomme*
24. Image Analysis Applications, *edited by Rangachar Kasturi and Mohan M. Trivedi*
25. Photoconductivity: Art, Science, and Technology, *N. V. Joshi*
26. Principles of Optical Circuit Engineering, *Mark A. Mentzer*
27. Lens Design, *Milton Laikin*
28. Optical Components, Systems, and Measurement Techniques, *Rajpal S. Sirohi and M. P. Kothiyal*
29. Electron and Ion Microscopy and Microanalysis: Principles and Applications, Second Edition, Revised and Expanded, *Lawrence E. Murr*

30. Handbook of Infrared Optical Materials, *edited by Paul Klocek*
31. Optical Scanning, *edited by Gerald F. Marshall*
32. Polymers for Lightwave and Integrated Optics: Technology and Applications, *edited by Lawrence A. Hornak*
33. Electro-Optical Displays, *edited by Mohammad A. Karim*
34. Mathematical Morphology in Image Processing, *edited by Edward R. Dougherty*
35. Opto-Mechanical Systems Design: Second Edition, Revised and Expanded, *Paul R. Yoder, Jr.*
36. Polarized Light: Fundamentals and Applications, *Edward Collett*
37. Rare Earth Doped Fiber Lasers and Amplifiers, *edited by Michel J. F. Digonnet*
38. Speckle Metrology, *edited by Rajpal S. Sirohi*
39. Organic Photoreceptors for Imaging Systems, *Paul M. Borsenberger and David S. Weiss*
40. Photonic Switching and Interconnects, *edited by Abdellatif Marrakchi*
41. Design and Fabrication of Acousto-Optic Devices, *edited by Akis P. Goutzoulis and Dennis R. Pape*
42. Digital Image Processing Methods, *edited by Edward R. Dougherty*
43. Visual Science and Engineering: Models and Applications, *edited by D. H. Kelly*
44. Handbook of Lens Design, *Daniel Malacara and Zacarias Malacara*
45. Photonic Devices and Systems, *edited by Robert G. Hunsperger*
46. Infrared Technology Fundamentals: Second Edition, Revised and Expanded, *edited by Monroe Schlessinger*
47. Spatial Light Modulator Technology: Materials, Devices, and Applications, *edited by Uzi Efron*
48. Lens Design: Second Edition, Revised and Expanded, *Milton Laikin*
49. Thin Films for Optical Systems, *edited by François R. Flory*
50. Tunable Laser Applications, *edited by F. J. Duarte*
51. Acousto-Optic Signal Processing: Theory and Implementation, Second Edition, *edited by Norman J. Berg and John M. Pellegrino*
52. Handbook of Nonlinear Optics, *Richard L. Sutherland*
53. Handbook of Optical Fibers and Cables: Second Edition, *Hiroshi Murata*
54. Optical Storage and Retrieval: Memory, Neural Networks, and Fractals, *edited by Francis T. S. Yu and Suganda Jutamulia*
55. Devices for Optoelectronics, *Wallace B. Leigh*
56. Practical Design and Production of Optical Thin Films, *Ronald R. Willey*
57. Acousto-Optics: Second Edition, *Adrian Korpel*
58. Diffraction Gratings and Applications, *Erwin G. Loewen and Evgeny Popov*
59. Organic Photoreceptors for Xerography, *Paul M. Borsenberger and David S. Weiss*
60. Characterization Techniques and Tabulations for Organic Nonlinear Optical Materials, *edited by Mark Kuzyk and Carl Dirk*

61. Interferogram Analysis for Optical Testing, *Daniel Malacara, Manuel Servín, and Zacarias Malacara*
62. Computational Modeling of Vision: The Role of Combination, *William R. Uttal, Ramakrishna Kakarala, Sriram Dayanand, Thomas Shepherd, Jagadeesh Kalki, Charles F. Lunskis, Jr., and Ning Liu*
63. Microoptics Technology: Fabrication and Applications of Lens Arrays and Devices, *Nicholas F. Borrelli*
64. Visual Information Representation, Communication, and Image Processing, *Chang Wen Chen and Ya-Qin Zhang*
65. Optical Methods of Measurement: Wholefield Techniques, *Rajpal S. Sirohi and Fook Siong Chau*
66. Integrated Optical Circuits and Components: Design and Applications, *edited by Edmond J. Murphy*
67. Adaptive Optics Engineering Handbook, *edited by Robert K. Tyson*
68. Entropy and Information Optics, *Francis T. S. Yu*
69. Computational Methods for Electromagnetic and Optical Systems, *John M. Jarem and Partha P. Banerjee*
70. Laser Beam Shaping: Theory and Techniques, *edited by Fred M. Dickey and Scott C. Holswade*
71. Rare-Earth-Doped Fiber Lasers and Amplifiers: Second Edition, Revised and Expanded, *edited by Michel J. F. Digonnet*
72. Lens Design: Third Edition, Revised and Expanded, *Milton Laikin*
73. Handbook of Optical Engineering, *edited by Daniel Malacara and Brian J. Thompson*
74. Handbook of Imaging Materials, *edited by Arthur S. Diamond and David S. Weiss*
75. Handbook of Image Quality: Characterization and Prediction, *Brian W. Keelan*
76. Fiber Optic Sensors, *edited by Francis T. S. Yu and Shizhuo Yin*
77. Optical Switching/Networking and Computing for Multimedia Systems, *edited by Mohsen Guizani and Abdella Battou*
78. Image Recognition and Classification: Algorithms, Systems, and Applications, *edited by Bahram Javidi*
79. Practical Design and Production of Optical Thin Films: Second Edition, Revised and Expanded, *Ronald R. Willey*
80. Ultrafast Lasers: Technology and Applications, *edited by Martin E. Fermann, Almantas Galvanauskas, and Gregg Sucha*

Additional Volumes in Preparation

Light Propagation in Periodic Media: Differential Theory and Design, *Michel Nevière and Evgeny Popov*

Optical Remote Sensing: Science and Technology, *Walter Egan*

ULTRAFAST LASERS

Technology and Applications

edited by

Martin E. Fermann
IMRA America, Inc.
Ann Arbor, Michigan, U.S.A.

Almantas Galvanauskas
University of Michigan
Ann Arbor, Michigan, U.S.A.

Gregg Sucha
IMRA America, Inc.
Ann Arbor, Michigan, U.S.A.

MARCEL DEKKER

MARCEL DEKKER, INC. NEW YORK • BASEL

Transferred to Digital Printing 2005

ISBN: 0-8247-0841-5

Headquarters
Marcel Dekker, Inc.
270 Madison Avenue, New York, NY 10016
tel: 212-696-9000; fax: 212-685-4540

Eastern Hemisphere Distribution
Marcel Dekker AG
Hutgasse 4, Postfach 812, CH-4001 Basel, Switzerland
tel: 41-61-260-6300; fax: 41-61-260-6333

World Wide Web
http://www.dekker.com

The publisher offers discounts on this book when ordered in bulk quantities. For more information, write to Special Sales/Professional Marketing at the headquarters address above.

Current printing (last digit):
10 9 8 7 6 5 4 3 2 1

Foreword

For over a decade, the ultrafast (sub-100 fsec) dye laser served as the workhorse of research laboratories from its invention in 1981 until the advent of the Ar^+-pumped Ti:sapphire laser in 1992. As a graduate student working in the early 1990s in the Picosecond Ultrasonics Group under Humphrey Maris at Brown University, I learned first-hand the benefits that this solid-state laser brought to our pump-probe experiments. We used ultrashort light pulses to generate sub-THz acoustic waves and study their propagation in various materials. Relative to the dye lasers available at that time, the Ti:sapphire possessed lower noise, higher power, and greater environmental stability, and this opened up several new directions for ultrafast research in our group.

Second-generation Ti:sapphire technology further led to and enabled commercialization of the picosecond ultrasonics technique in 1998. Teams at Rudolph Technologies Inc. (RTEC) and Coherent, Inc., worked closely to develop the Vitesse™, à turnkey solid-state-pumped Ti:sapphire laser specifically designed for use in RTEC's MetaPULSE™ thin-film metrology system. The MetaPULSE is a highly automated system that has been widely adopted by manufacturers of microprocessors, DRAM, and magnetic storage for on-product thickness measurement of metal films ranging from several microns down to 20 angstroms in thickness. In 2001, RTEC announced the sale of its 100th MetaPULSE, representing a laser market of over \$3 million per year since the product's introduction.

Three characteristics of the solid-state-pumped Ti:sapphire laser have proved instrumental to its industrial success: simple facilities requirements, compact size, and excellent stability. These improvements all result largely from replacing the Ar^+ pump with a Nd:vanadate laser. The all solid-state pump laser is highly efficient, permitting it to be plugged into a normal electrical outlet and resulting in a rate of heat generation lower than that of the average household lightbulb. Compact size is a key factor in product success in the semiconductor-manufacturing environment because of the high costs associated with building and maintaining a Class 1 cleanroom space. Laser stability and long lifetime are also essential in the semiconductor industry, in which equipment uptime in excess of 95% is standard in a 24 hours/7 days mode of operation. Coherent, Inc., designed the Vitesse with a highly stable, folded Ti:sapphire cavity, actively PZT-steered pump beam, and diode current servo loop for reliable hands-off laser operation over months or years. The latest product design refinements and increasing industry competition will have the result of extending the hands-off Ti:sapphire lifetime to greater than 10,000 hours by 2003, representing a stability improvement of nearly five orders of magnitude as compared with the ultrafast dye lasers of the early 1990s.

Thin-film semiconductor process metrology represents just one of many potential high-volume industrial applications for ultrafast lasers. The high market value of microprocessors and memory devices, at least in the near term, can support the typical $100,000 Ti:sapphire price tag over a limited number of process control tools (6–10 per manufacturing line). The same cannot be said for other potential markets: one timely example within the semiconductor industry is integrated metrology. In contrast to the stand-alone metrology model, in the integrated approach the metrology tool is "on board" with each process tool; in the case of an integrated MetaPULSE, a metal film deposition or polishing system would be the most likely target for integration. While integrated metrology has several potential pitfalls and it is still too early to accurately predict the future market size, the approach may improve process tool uptime and the semiconductor product yield by shortening the loop, or adding feedback, between the process step and its control measurement. For a typical semiconductor process step, a standalone metrology tool may serve around five process tools; thus the market for integrated MetaPULSE units is potentially up to five times larger than the standalone market. Market analysis shows, however, that to be accepted and cost-effective, integrated metrology will likely require the equipment cost (including the laser) to decrease by at least the same factor (or down to $10,000– $20,000 or less). In addition, when metrology is placed inside a process tool, this requires a higher demand on laser compactness and reliability. Hands-off laser lifetimes greater than 10,000 hours will become an even greater necessity because failure of an integrated metrology tool leads to downtime of the process tool, thereby impeding the production line. These cost, compactness, and reliability considerations may lead to greater adoption of fiber-based ultrafast lasers in the near future as the market develops for integrated metrology.

Laser price performance points (e.g., pulse duration, power, wavelength, and noise) will, in general, be highly application-dependent; therefore, the industrial market for ultrafast lasers will most likely be split between different technologies and suppliers. For example, laser micromachining is already an established market with laser power, pulse duration, and wavelength requirements significantly different from those of nondestructive testing. At five years old the industrial ultrafast laser market is still in its infancy, and a rapidly growing market is plausible over the next decade as new industrial applications continue to emerge.

Christopher J. Morath
Rudolph Technologies, Inc.
Flanders, New Jersey

Preface

With the wide availability of commercial ultrafast laser systems, their applications to many areas of science and industry are blossoming. Indeed, ultrafast technology has diversified to such an extent that a comprehensive review of the whole field is nearly impossible. On the one hand, ultrafast lasers have entered the world of solid commerce; on the other, they continue to lead to breathtaking advances in areas of fundamental science.

The high degree of maturity that ultrafast optics has achieved in many areas inspired us to compile this book on selected topics in some of the most prominent areas. In selecting research topics, we concentrated on areas that have indeed already experienced a transformation to the commercial side of things, or where such a transformation is currently evolving or can at least be anticipated in the not too distant future, although, of course, we do not claim to predict where the field of ultrafast optics is heading. The only certainty is that ultrafast lasers will continue to play a rapidly growing role in technology with the so far elusive mass applications looming on the horizon.

Ultrafast Lasers is intended for researchers, engineers, and graduate students who are interested in a review of ultrafast optics technology. It consists of two parts, with the first describing some of the most widely used ultrafast laser systems and the second describing some of the best-known applications. On the laser systems side we cover ultrafast solid-state fiber, and diode lasers, and on the applications side we provide a general overview before presenting specific topics ranging from biology, electronics, optical communications, and mechanical engineering to integrated optics.

This book addresses the reader who is interested in a summary of the unique capabilities of ultrafast lasers. We hope that by providing this broad overview, we can contribute to the rapid advancement of a truly exciting technology.

Martin E. Fermann
Almantas Galvanauskas
Gregg Sucha

Contents

Contributors

A. Apolonski Technische Universität Wien, Vienna, Austria
Mark Brezinski Massachusetts Institute of Technology, Cambridge, Massachusetts, U.S.A.
Qin Chen Rensselaer Polytechnic Institute, Troy, New York, U.S.A.
Peter J. Delfyett University of Central Florida, Orlando, Florida, U.S.A.
Wolfgang Drexler Massachusetts Institute of Technology, Cambridge, Massachusetts, U.S.A.
Martin E. Fermann IMRA America, Inc., Ann Arbor, Michigan, U.S.A.
James G. Fujimoto Massachusetts Institute of Technology, Cambridge, Massachusetts, U.S.A.
Almantas Galvanauskas University of Michigan, Ann Arbor, Michigan, U.S.A.
José F. García Harvard University, Cambridge, Massachusetts, U.S.A.
T. W. Hänsch Max-Planck-Institut für Quantenoptik, Garching, Germany
Ingmar Hartl Massachusetts Institute of Technology, Cambridge, Massachusetts, U.S.A.
R. Holzwarth Max-Planck-Institut für Quantenoptik, Garching, Germany
Alan O. Jamison Harvard University, Cambridge, Massachusetts, U.S.A.
Tibor Juhasz University of Michigan, Ann Arbor, Michigan, U.S.A.
Franz Kärtner Massachusetts Institute of Technology, Cambridge, Massachusetts, U.S.A.
Ursula Keller Swiss Federal Institute of Technology, Zurich, Switzerland
F. Krausz Technische Universität Wien, Vienna, Austria
Ronald M. Kurtz University of California at Irvine, Irvine, California, U.S.A.
Xingde Li Massachusetts Institute of Technology, Cambridge, Massachusetts, U.S.A.
Eric Mazur Harvard University, Cambridge, Massachusetts, U.S.A.
Uwe Morgner Massachusetts Institute of Technology, Cambridge, Massachusetts, U.S.A.
Michiel Müller University of Amsterdam, Amsterdam, The Netherlands
Masataka Nakazawa Tohoku University, Miyagi-ken, Japan

Stefan Nolte Friedrich Schiller University, Jena, Germany
Rüdiger Paschotta Swiss Federal Institute of Technology, Zurich, Switzerland
François Salin Université Bordeaux I, Talence, France
Melvin A. Sarayba University of California at Irvine, Irvine, California, U.S.A.
Chris B. Schaffer Harvard University, Cambridge, Massachusetts, U.S.A.
Jeff Squier Colorado School of Mines, Golden, Colorado, U.S.A.
Gregg Sucha IMRA America, Inc., Ann Arbor, Michigan, U.S.A.
G. Tempea Technische Universität Wien, Vienna, Austria
J. F. Whitaker University of Michigan, Ann Arbor, Michigan, U.S.A.
K. Yang University of Michigan, Ann Arbor, Michigan, U.S.A.
X.-C. Zhang Rensselaer Polytechnic Institute, Troy, New York, U.S.A.

ULTRAFAST LASERS

1
Ultrafast Solid-State Lasers

Rüdiger Paschotta and Ursula Keller
Swiss Federal Institute of Technology, Zurich, Switzerland

1.1 INTRODUCTION

Since 1990 we have observed tremendous progress in picosecond and femtosecond pulse generation using solid-state lasers. Today ultrashort-pulse lasers are normally based on solid-state lasers, which provide sufficiently high average powers to efficiently generate many other frequencies with nonlinear frequency conversion schemes such as second harmonic to high harmonic generation, optical parametric oscillation, and amplification. The emphasis of this chapter is to give an updated review of the progress in pulsed solid-state lasers during the last ten years. Our goal is to give also to the non-expert an efficient starting point to enter into this field without providing all the detailed derivations. Relevant and useful references for further information are provided throughout the chapter.

For ultrashort-pulse generation we usually rely on continuous-wave (cw) mode locking, where the laser gain medium is pumped continuously and many axial laser modes are locked together in phase to form a short pulse. A homogeneously broadened laser would often lase in only one axial mode. In a modelocked laser, additional energy is transferred with the correct phase to adjacent modes with either active loss or a phase modulator (for active modelocking) or passive self-amplitude modulation (SAM) (for passive modelocking) inside the laser cavity. In the time domain, the many phase-locked axial modes result in a short pulse of a duration inversely proportional to the spectral width of all the phase-locked axial modes. Generally, passive modelocking generates shorter pulses and is much simpler than active modelocking. For reliable passive cw modelocking, the pulse generation starts from normal laser noise within less than approximately 1 ms. The required SAM is typically obtained with a saturable absorber in the laser cavity. A saturable absorber is a device that has a lower loss for higher pulse intensities or energies. This can occur, for example, when the initial states of the absorbing transition are emptied or when the final states are occupied. The interaction of a short pulse with such a saturable absorber then produces a self-amplitude modulation due to the intensity-dependent absorption. For modelocking, the resulting pulses are typically much shorter than the cavity round-trip time, and the pulse repetition rate (typically between a few tens of megahertz and tens of gigahertz) is determined by the cavity round-trip time. Under certain conditions, the pulse repetition rate can be some integer multiple of the fundamental repetition rate; this is called harmonic modelocking (Becker et al., 1972).

Modelocking was first demonstrated in the mid-1960s using a HeNe laser (Hargrove et al., 1964), a ruby laser (Mocker and Collins, 1965), and an Nd:glass laser (De Maria et al., 1966). However, at the time passively modelocked solid-state lasers were also Q-switched. In this regime, called Q-switched modelocking (Fig. 1), the modelocked picosecond or femtosecond pulses are modulated with a much longer Q-switched pulse envelope (typically in the microsecond regime), which occurs at a much lower repetition rate (typically in the kilohertz regime). This continued to be a problem for most passively modelocked solid-state lasers until in 1992 the first intracavity saturable absorber was designed correctly to prevent self-Q-switching instabilities in solid-state lasers with microsecond or even millisecond upper-state lifetimes (Keller et al., 1992a).

For some time, the success of ultrafast dye lasers in the 1970s and 1980s diverted research interest away from solid-state lasers. Q-switching instabilities are not a problem for dye lasers. In 1974 the first subpicosecond passively modelocked dye lasers (Shank and Ippen, 1974; Ruddock and Bradley, 1976; Diels et al., 1978) and in 1981 the first sub-100 fs colliding pulse modelocked (CPM) dye lasers (Fork et al., 1981) were demonstrated. The CPM dye laser was the "workhorse" all through the 1980s for ultrafast laser spectroscopy in physics and chemistry. This CPM dye laser produced pulses as short as 27 fs with a typical average output power of about 20 mW (Valdmanis et al., 1985). The wavelength was centered around 630 nm and was not tunable. Shorter pulse durations, down to 6 fs, were achieved only through additional amplification and external pulse compression at much lower repetition rates (Fork et al., 1987).

The development of diode lasers with higher average powers in the 1980s again stimulated strong interest in solid-state lasers. Diode laser pumping provides dramatic improvements in efficiency, lifetime, size, and other important laser characteristics. For example, actively modelocked diode-pumped Nd:YAG (Maker and Ferguson, 1989a) and Nd:YLF

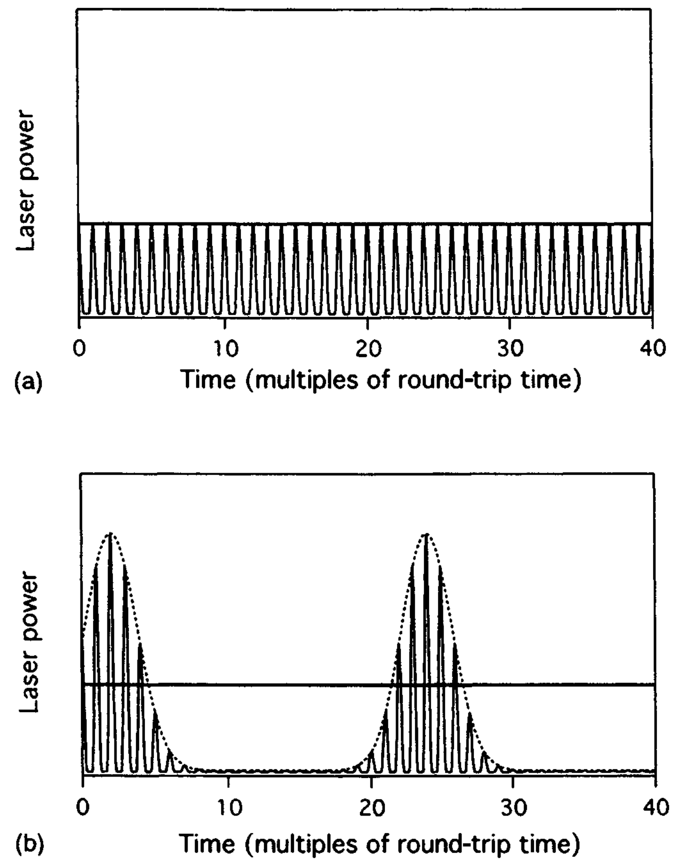

Figure 1 Schematic illustration of (a) continuous-wave (cw) modelocking and (b) Q-switched modelocking.

(Maker and Ferguson, 1989b; Keller et al., 1990a; Weingarten et al., 1990; Juhasz et al., 1990) lasers generated 7–12 ps pulse durations for the first time. In comparison, flashlamp-pumped Nd:YAG and Nd:YLF lasers typically produced pulse durations of ~100 ps and ~30 ps, respectively. Before 1992, however, all attempts to passively modelock diode-pumped solid-state lasers resulted in Q-switching instabilities that at best produced stable modelocked pulses within longer Q-switched macropulses, as mentioned above.

The breakthrough of ultrafast solid-state lasers happened with the discovery of the Ti:sapphire lase medium (Moulton, 1986), which was the first solid-state laser medium that was able to support ultrashort pulses without cryogenic cooling. The existing passive modelocking techniques, primarily developed for dye lasers, were inadequate because of the much longer upper-state lifetime (i.e., in the microsecond regime) and smaller gain cross section (i.e., in the $10^{-19}\,cm^2$ regime) of Ti:sapphire compared to dyes (i.e., in the nanosecond and $10^{-16}\,cm^2$ regimes). Therefore, passive pulse generation techniques had to be re-evaluated with new laser material properties in mind. The strong interest in an all-solid-state ultrafast laser technology was the driving force and formed the basis for many new inventions and discoveries.

Kerr lens modelocking (KLM) (Spence et al., 1991) of Ti:sapphire lasers was discovered in 1991 and produced the shortest laser pulses—pulses of less than 6 fs duration (Sutter et al., 1999; Morgner et al., 1999a, 1999b)—directly from the laser cavity without any additional external cavity pulse compression. Slightly shorter sub-5 fs pulses have been demonstrated with external pulse compression (Baltuska et al., 1997; Nisoli et al., 1997) and continuum generation together with parametric optical amplification (Shirakawa et al., 1999). Although very different in technical detail, all of these sub-6 fs pulse generation techniques rely on the same three main components: nonlinear Kerr effect, higher order dispersion control, and ultrabroadband amplification (Steinmeyer et al., 1999). KLM, however, has serious limitations because the modelocking process is generally not self-starting and critical cavity alignment close to the cavity stability limit is required to obtain stable pulse generation. Thus, the laser cavity has to be optimized for the best pulse shaping and not necessarily for the best efficiency and the greatest output power. This sets serious constraints on the cavity design, which become even more severe at higher average output powers and for more compact monolithic cavities. Thus, passively mode-locked solid-state lasers using intracavity semiconductor saturable absorber mirrors (SESAMs) have become a very attractive alternative to KLM.

In 1992, semiconductor saturable absorber mirrors (SESAMs) (Keller et al., 1992a; 1996) allowed for the first time self-starting and stable passive modelocking of diode-pumped solid-state lasers with an intracavity saturable absorber. The design freedom of SESAMs allowed for a systematic investigation of the stability regimes of passive Q-switching and passive cw modelocking with an improved understanding and modeling of Q-switching (Hönninger et al., 1999a) and multiple pulsing instabilities (Aus der Au et al., 1997; Kärtner et al., 1998). Simple laser and SESAM design guidelines allowed us to continue to push the frontiers of ultrafast solid-state lasers during the last ten years. Presently, the frontiers in average output power of diode-pumped solid-state lasers are set in the picosecond regime with Nd:YAG lasers (27 W average output power and 19 ps pulse duration) (Spühler et al., 2000) and in the femtosecond regime with Yb:YAG lasers (16 W, 730 fs) (Aus der Au et al., 2000). This basically means that microjoule-level pulse energies in both the picosecond and femtosecond regimes are available directly from compact solid-state lasers without cavity dumping or further pulse amplification. In addition, the frontier in pulse repetition rate has been recently pushed to nearly 80 GHz by the use of quasi-monolithic miniature Nd:YVO_4 laser cavities (Krainer et al., 2000). Today SESAMs are well established for ultrafast all-solid-state lasers. The main reason for this device's utility is that both the linear and nonlinear optical properties can be engineered over a wide range, allowing for more freedom in the specific laser cavity design. The main absorber parameters such as operation wavelength, modulation depth, saturation fluence, and absorber lifetime can be custom designed for stable cw modelocking or Q-switching. Initially, semiconductor saturable absorber mirrors were used in coupled cavities (Keller et al., 1990b), because they introduced too much loss inside solid-state lasers with small gain cross sections (i.e., $10^{-19}\,\mathrm{cm}^2$ and smaller). Two years later, in 1992, this work resulted in a new type of intracavity saturable absorber mirror, the antiresonant Fabry-Perot saturable absorber (A-FPSA) (Keller et al., 1992a), where the absorber was integrated inside a Fabry-Perot structure of which the bottom reflector was a high reflector (with nearly 100% reflectivity). The Fabry-Perot was operated at antiresonance to obtain broad bandwidth and low loss. The A-FPSA mirror was based on a semiconductor Bragg mirror, an absorber layer, and a dielectric top reflector and therefore allowed for a large variation of the absorber parameters. The result was a much better understanding of the absorber and laser design necessary to obtain stable passive mode locking or Q-switching of many different solid-state lasers. Scaling of the A-FPSA design resulted in a semiconductor Bragg mirror with only one single-quantum-well saturable absorber layer (Brovelli et al., 1995; Jung et al., 1995a). This design was later also referred to as a saturable Bragg reflector (SBR) (Tsuda et al., 1995). In 1995, it was further realized that the intracavity saturable absorber can be integrated into a more general mirror structure that allows for both saturable absorption and negative dispersion control, which is now generally referred to as a SESAM. In a general sense, then, we can reduce the design problem of a SESAM to the analysis of multilayer interference filters for a given desired nonlinear reflectivity response for both the amplitude and phase. Thus, if required, the SESAM provides not only saturable absorption but also negative dispersion compensation. The A-FPSA, and SBR, and the dispersive saturable absorber mirror (D-SAM) (Kopf et al., 1996a) are therefore special examples of SESAM designs. A more detailed summary of different SESAM designs is given in a recent book chapter (keller, 1999).

A new modelocking technique, referred to as soliton modelocking (Kärtner and Keller, 1995; Jung et al., 1995b; Kärtner et al., 1996), totally removes the cavity design constraints of KLM lasers and substantially relaxes the requirements of the SESAM performance in the femtosecond regime. The pulse formation is basically done by the soliton effects, and the saturable absorber is required only to start and stabilize the modelocking. Thus, even a SESAM with a relatively long recovery time can support very short pulses. For example, a SESAM with a recovery time of 10 ps was sufficient to stabilize soliton pulses of only 300 fs duration in a Ti:sapphire laser (Jung et al., 1995b). In contrast to KLM, no critical cavity alignment is necessary and modelocking is self-starting. Pulses as short as 13 fs have been produced with soliton modelocked Ti:sapphire lasers (Kärtner et al., 1996).

Today, a large variety of reliable and compact all-solid-state ultrafast lasers are available with pulse durations ranging from picoseconds to less than 100 fs. Table 1 summarizes the results achieved for various solid-state lasers and various modelocking (ML) techniques. For each technique we provide the first demonstration and the best results. A more detailed table with all results is provided elsewhere (Keller, 2001). For each laser material we emphasize the best results in terms of pulse duration, average outpur power, and pulse repetition rates with bold letters. For completeness we also include the coupled-cavity modelocking (CCM) techniques even though they have become less relevant today because SESAM-based ultrafast lasers are much simpler and more compact. We distinguish between two different CCM techniques: Additive pulse modelocking (APM) is a coupled-cavity modelocking technique for which the coupled cavity generates a nonlinear phase shift that adds constructively at the peak of the pulse inside the main cavity and destructively in the wings, thus shortening the pulse duration inside the main cavity. This was first discovered by Kean et al. (1989) and later explained in this simple model by Ippen et al. (1989). However, APM requires interferometric cavity length stabilization of the coupled cavity. Resonant passive modelocking (RPM) (Keller et al., 1990b; Haus et al., 1991) removed this problem by using an amplitude nonlinearity inside the coupled cavity.

This chapter is organized as follows. In Section 1.2 we discuss the demands on gain media for ultrashort-pulse generation and give an overview on available media as well as the corresponding achievements. Sections 1.3 and 1.4 are devoted to technical issues of particular importance, namely the effects of dispersion and nonlinearities in laser cavities and different modelocking techniques. Several examples for ultrafast lasers are then discussed in Section 1.5. Although ultrafast pulses are usually generated with modelocked lasers, in Section 1.6 we also discuss a kind of Q-switched laser that can generate picosecond pulses. Finally, we give a short summary and outlook in Section 1.7.

Table 1. Continuous-Wave Modelocked Solid-State Lasers Using Different Modelocking Techniques[a]

Laser material	ML technique	λ_0	τ_p	$P_{av,out}$	f_{rep}	Remarks	Ref.
Ti:sapphire							
	Active AOM	814 nm	150 fs	600 mW	80.5 MHz		Curley and Ferguson, 1991
	CCM-APM		1.4 ps	300 mW		Highly chirped 1.4 ps output pulses, externally compressed down to 200 fs	Goodberlet et al., 1989
	CCM-RPM	860 nm	2 ps	90 mW	250 MHz		Keller et al., 1990b
	Dye sat. absorber	750 nm	140 fs			KLM started with dye-saturable absorber (not understood—assumed to have a CPM Ti:sapphire laser)	Sarukura et al., 1991
	KLM	880 nm	60 fs	300 mW		First demonstration of KLM (but KLM not understood)	Spence et al., 1991
		~800 nm	**<6 fs**	300 mW	85 MHz	Fused silica prisms and double-chirped mirrors, KLM is self-starting with SESAM	Sutter et al., 1999

(*Continued*)

Laser material	ML technique	λ_0	τ_p	$P_{av,out}$	f_{rep}	Remarks	Ref.
		~800 nm	**<6 fs**	200 mW	90 MHz	CaF_2 prisms, double-chirped mirrors	Morgner et al., 1999b
		780 nm	8.5 fs	**1 W**	75 MHz	1.5 MW peak, focused intensity $5 \times 10^{13}\,W/cm^2$	Xu et al., 1998
		850 nm	13 fs	**1.5 W**	110 MHz	1 MW peak, 13 nJ out	Beddard et al., 1999
		800 nm	16.5 fs	170 mW	**15 MHz**	0.7 MW peak	Cho et al., 1999
		782 nm	23 fs	300 mW	**2 GHz**	Ring laser, self-starting modelocking due to feedback from external mirror	Bartels et al., 1999
	Soliton-SESAM	840 nm	34 fs	140 mW	98.9 MHz	First SESAM design with a single quantum well absorber in a Bragg reflector	Brovelli et al., 1995
		810 nm	13 fs	80 mW	85 MHz	Shortest pulse with soliton modelocking and no KLM	Kärtner et al., 1996

Cr:LiSAF							
	KLM	800–880 nm	150 fs	50 mW	82 MHz	First modelocked femtosecond Cr:LiSAF laser, Kr-pumped	Miller et al., 1992
			300 ps	~1 mW		**First** diode-pumped modelocked Cr:LiSAF laser, AOM or RPM for starting KLM	French et al., 1993
			220 fs	~10 mW		KLM started by SESAM	Mellish et al., 1994
		850 nm	**12 fs**	23 mW	200 MHz	ML not self-starting	Uemura et al., 1999
	Soliton-SESAM	840 nm	98 fs	50 mW	120 MHz	**First** soliton mode-locking, no KLM required	Kopf et al., 1994a
		850 nm	45 fs	105 mW	176 MHz		Kopf et al., 1995a
		875 nm	110 fs	**500 mW**	150 MHz	Low-brightness 0.9 cm wide, 15 W diode laser array	Kopf et al., 1997
Cr:LiCAF							
	KLM	800 nm	170 fs	100 mW	90 MHz	Kr-pumped	LiKamWa et al.,1992
		820 nm	**20 fs**	13 mW	95 MHz		Gabel et al., 1998
Cr:LiSGaF							
	KLM	830 nm	100 fs (50 fs)	35 mW	71 MHz		Yanovsky et al., 1995
		895 nm	**14 fs**	100 mW	70 MHz	Kr ion laser pumped, chirped mirror	Sorokina et al., 1997
	Soliton-SESAM	839 nm	61 fs	78 mW	119 MHz		Loesel et al., 1997

(Continued)

Laser material	ML technique	λ_0	τ_p	$P_{av,out}$	f_{rep}	Remarks	Ref.
Cr:LiSCAF							
	KLM	860 nm	90 fs	100 mW	140 MHz	Kr-ion-laser pumped	Wang et al., 1994
Cr:Forsterite	KLM	1.23 μm (1.21–1.27 μm)	48 fs	380 mW	81 MHz	Nd:YAG laser pumped, KLM self-starting with AOM	Sennaroglu et al., 1993
		1.3 μm	**14 fs**	80 mW	100 MHz	Double chirped mirrors	Chudoba et al., 2000
	Soliton-SESAM	1.29 μm	40 fs	60 mW		$Nd:YVO_4$ laser pumped	Zhang et al., 1997a
		1.29 μm	36 fs	60 mW		$Nd:YVO_4$ laser pumped	Zhang et al., 1997b
		1.26 mW	78 fs	**800 mW**	83 MHz	Nd:YAG laser pumped	Petrov et al., 1998
Cr:YAG							
	KLM	1.52 μm	120 fs	360 mW	81 MHz	Nd:YAG laser pumped, regen. AOM for starting KLM	Sennaroglu et al., 1994
		1.54 μm	**43 fs**	200 mW	70 MHz	$Nd:YVO_4$ laser pumped	Tong et al., 1997
		1.52 μm	55 fs		**1.2 GHz**	$Nd:YVO_4$ laser pumped	Tomaru et al., 2000
	Soliton-SESAM	1.541 μm	110 fs	70 mW		$Nd:YVO_4$ laser pumped	Collings et al., 1996
		1.52 μm	**44 fs**	65 mW		$Nd:YVO_4$ laser pumped	Zhang et al., 1999

Nd:YAG							
	Active AOM	1.064 μm	25 ps			Lamp-pumped: pulse shortening due to intracavity etalon	Roskos et al., 1986
	Active FM	1.064 μm	12 ps	65 mW	350 MHz		Maker et al., 1989a
	Active EOM	1.32 μm	8 ps	240 mW	**1 GHz**		Zhou et al., 1991
	Active AOM	1.32 μm	53 ps	1.5 W	200 MHz	Lamp-pumped and harmonically modelocked	Keller et al., 1988
	CCM-APM	1.064 μm	**1.7 ps**	25 mW	136 MHz		Goodberlet et al., 1990
		1.32 μm	10 ps	700 mW	100 MHz	Lamp-pumped	Liu et al., 1990a
	KLM	1.064 μm	8.5 ps	1 W	100 MHz		Liu et al., 1992
		1.064 μm	**6.7 ps**	675 mW	106 MHz	Ti:sapphire laser-pumped	Henrich and Beigang, 1997
	SESAM	1.064 μm	8.7 ps	100 mW	100 MHz		Weingarten et al., 1993
		1.064 μm	**6.8 ps**	400 mW	217 MHz		Keller, 1994
		1.064 μm	19 ps	27 W	55 MHz	Three side-pumped laser heads	Spühler et al., 2000
	Polarization switching in nonlinear crystal	1.064 μm	23 ps	4 W	150 MHz	Lamp-pumped, KTP crystal	Kubecek et al., 1999

(Continued)

Laser material	ML technique	λ_0	τ_p	$P_{av,out}$	f_{rep}	Remarks	Ref.
Nd:YLF							
	Active AOM	1.053 μm	37 ps	6.5 W	100 MHz	Laser-pumped	Bado et al., 1987
		1.053 μm	18 ps	12 mW	230 MHz		Maker and Ferguson, 1989c
		1.047 μm	7 ps	135 mW	2 GHz		Weingarten et al., 1990
		1.047 μm	6.2 ps	20 mW	1 GHz	Ti:sapphire laser-pumped	Walker et al., 1990
	Active FM	1.053 μm	4.5 ps	400 mW	**2.85 GHz**		Weingarten et al., 1992
		1.3 μm	8 ps	240 mW	1 GHz		Zhou et al., 1991
	KLM	1.047 μm	3 ps	250 mW			Lincoln and Ferguson, 1994
		1.047 μm	2.3 ps	800 mW	82 MHz	Lamp-pumped, microdot mirror	Ramaswamy et al., 1993
	SESAM	1.047 μm	3.3 ps	700 mW	220 MHz	Ti:sapphire laser-pumped	Keller et al., 1992a
		1.047 μm	2.8 ps	460 mW	220 MHz		Keller, 1994
		1.3 μm	5.7 ps	130 mW	98 MHz		Fluck et al., 1996
	CCM-APM	1.053 μm	3.7 ps	7 W	76 MHz	Lamp-pumped	Liu and Chee, 1990b
		1.053 μm	1.7 ps		103 MHz		Jeong et al., 1999
		1.047 μm	**1.5 ps**	20 mW	123 MHz		Malcolm et al., 1990
	CCM-RPM	1.047 μm	3.7 ps	550 mW	250 MHz	Ti:sapphire laser-pumped	Keller et al., 1992b

Nd:YVO_4							
	SESAM	1.064 μm	7 ps	4.5 W	84 MHz		Ruffing et al., 1997
		1.064 μm	21 ps	**20 W**	90 MHz		Burns et al., 2000
		1.064 μm	**2.7 ps**	65 mW	**77 GHz**	Ti:sapphire laser pumped	Krainer et al., 2000
		1.3 μm	4.6 ps	50 mW	93 MHz		Fluck et al., 1996
	Nonlinear mirror ML	1.064 μm	7.9 ps	1.35 W	150 MHz		Agnesi et al., 1997
	Intensity-dependent polarization rotation	1.064 μm	**2.8 ps**	670 mW	130 MHz		Couderc et al., 1999
Nd:LSB							
	SESAM	1.062 μm	**1.6 ps**	210 mW	240 MHz	Ti:sapphire laser-pumped	Braun et al., 1996
		1.062 μm	2.8 ps	400 mW	177 MHz		Braun et al., 1996
Nd:BEL							
	Active-AOM	1.070 μm	7.5 ps	230 mW	250 MHz		Li et al., 1991
	Active-Fm	1.070 μm	**2.9 ps**	30 mW	238 MHz	Harmonic mode locking	Godil et al., 1991
		1.070 μm	3.9 ps	30 mW	**20 GHz**[3]	Harmonic mode locking	Godil et al., 1991
Nd:glass							
Nd:phosphate	Active-AOM	1.054 μm	7 ps	20 mW		Ar ion laser-pumped	Yan et al., 1986
		1.054 μm	~10 ps	30 mW			Basu and Byer, 1988
		1.054 μm	9 ps	30 mW	240 MHz		Hughes et al., 1992

(Continued)

Laser material	ML technique	λ_0	τ_p	$P_{av,out}$	f_{rep}	Remarks	Ref.
		1.063 µm	310 fs	70 mW	240 MHz	Ti:sapphire laser-pumped, regeneratively actively modelocked	Kopf et al., 1994b
Nd:phosphate glass	Active-FM	1.054 µm	9 ps	14 mW	235 MHz		Hughes et al., 1991
Nd:phosphate glass	CCM-APM	1.054 µm	122 fs	200 mW		Kr ion laser-pumped	Spielmann et al., 1991
Nd:phosphate glass	Soliton-SESAM	1.054 µm	150 fs	110 mW	180 MHz		Kopf et al., 1995b
		1.054 µm	120 fs	30 mW	150 MHz	Single prism for dispersion compensation	Kopf et al., 1996b
		1.054 µm	275 fs	**1.4 W**	74 MHz		Paschotta et al., 2000a
Nd:fluoro-phosphate glass		1.065 µm	**60 fs**	84 mW	114 MHz		Aus der Au et al., 1997
Nd:silicate		1.064 µm	130 fs	80 mW	180 MHz		Kopf et al., 1995b
Yb:YAG							
	Soliton-SESAM	1.03 µm	540 fs	100 mW	81 MHz	First passively modelocked Yb:YAG laser	Hönninger et al., 1995

		1.03 μm	**340 fs**	170 mW		Hönninger et al., 1999b
		1.03 μm	730 fs	**16.2 W**	35 MHz	Aus der Au et al., 2000
Yb:KGW						
	Soliton-SESAM	1.037 μm	176 fs (112 fs)	1.1 W (0.2 W)	86 MHz	Brunner et al., 2000
Yb:GdCOB						
	Soliton-SESAM	1.045 μm	90 fs	40 mW	100 MHz	Druon et al., 2000
Yb:glass						
Yb:phosphate glass	Soliton-SESAM	1.025–1.065 μm	58 fs	65 mW	112 MHz	Hönninger et al., 1998
Yb:silicate glass		1.03–1.082 μm	61 fs	53 mW	112 MHz	Hönninger et al., 1998

[a] "Best" means in terms of pulse duration, highest average output power, highest pulse repetition rate etc. The result for which "best" applies is in bold letters. The lasers are assumed to be diode-pumped, if not stated otherwise (except Ti:sapphire laser). **ML** = modelocking; **CCM** = coupled-cavity modelocking; **APM** = additive pulse modelocking; **RPM** = resonant passive modelocking; **KLM** = Kerr lens modelocking; **SESAM** = semiconductor saturable absorber mirror; **soliton-SESAM** = soliton modelocking with a SESAM; **SESAM** = saturable absorber modelocking using SESAMs; **AOM** = acousto-optic modulator; **EOM** = electro-optic phase modulator; λ_0-center lasing wavelength; τ_p-measured pulse duration; $P_{av,out}$-average output power; f_{rep}-pulse repetition rate.

1.2 GAIN MEDIA FOR ULTRASHORT-PULSE GENERATION

Gain media for ultrafast lasers have to meet a number of conditions. We first list those criteria that apply to continuous-wave (cw) lasers as well. Obviously the gain medium should have a laser transition in the desired wavelength range and a pump transition at a wavelength where a suitable pump source is available. Several factors are important to achieve good power efficiency: a small quantum defect, the absence of parasitic losses, and a high gain ($\sigma\tau$ product) are desirable. The latter allows for the use of an output coupler with relatively high transmission, which makes the laser less sensitive to intracavity losses. For high-power operation, we prefer media with good thermal conductivity, a week (or even negative) temperature dependence of the refractive index (to reduce thermal lensing), and a week tendency to undergo thermally induced stress fracture.

For ultrafast lasers, in addition we require a broad emission bandwidth, because ultrashort pulses intrinsically have a large bandwidth. More precisely, we need a large range of wavelengths in which a smooth gain spectrum is obtained for a fixed inversion level. The latter restrictions explain why the achievable modelocked bandwidth is in some cases [e.g., some Yb^{3+}-doped media (Hönninger et al., 1999b)] considerably smaller than the tuning range achieved with tunable cw lasers, particularly for quasi-three-level gain media. A less obvious requirement is that the laser cross sections should be high enough. Although the requirement of a reasonably small pump threshold can be satisfied even with low laser cross sections if the fluorescence lifetime is large enough, it can be very difficult to overcome Q-switching instabilities (see Sec. 1.4.3) in a passively modelocked laser based on a gain material with small laser cross sections. Unfortunately, many broadband gain media tend to have small laser cross sections, which can significantly limit their usefulness for passive modelocking, particularly at high pulse repetition rates and in cases where the pump beam quality is poor, necessitating a large mode area in the gain medium. Finally, a short pump absorption length is desirable because it permits the use of a short path length in the medium, which allows for operation with a small mode area in the gain medium and also limits the effects of dispersion and Kerr nonlinearity.

Most ultrafast lasers belong to one of two groups. The first group is based on gain media that have quite favorable properties for diode-pumped high-power cw operation but cannot be used for femtosecond pulse generation because of their relatively small amplification bandwidth. Typical examples are Nd^{3+}:YAG and Nd^{3+}:YVO_4. With high-power laser diodes, one or several conventional end-pumped or side-pumped laser rods and a SESAM (Sec. 1.4.3) for modelocking, up to 27 W or average power in 20 ps pulses has been achieved with Nd^{3+}:YAG (Spühler et al., 2000) and

20 W in 20 ps pulses with $Nd^{3+}:YVO_4$ (Burns et al., 2000). Significantly shorter pulse durations have been achieved at lower output powers, down to 1.5 ps with 20 mW (Malcolm et al., 1990), using the technique of additive pulse modelocking (APM, Sec. 1.4.3). For all these Nd^{3+}-doped media the relatively large laser cross sections usually make it relatively easy to achieve stable modelocked operation without Q-switching instabilities. See Section 1.5.1 for typical cavity setups.

The second group of gain media are characterized by a much broader amplification bandwidth, typically allowing for pulse durations well below 0.5 ps but also usually by significantly poorer thermal properties and smaller laser cross sections. Ti^{3+}:sapphire (Moulton, 1986) is a notable exception, combining nearly all desired properties for powerful ultrafast lasers, except that the short pump wavelength excludes the use of high-power diode pump lasers and the quantum defect is large. Using an argon ion laser or a frequency-doubled solid-state laser as a pump source, Ti^{3+}:sapphire lasers have been demonstrated to generate pulses with durations below 6 fs and a few hundred milliwatts of average power (Sutter et al., 1999; Morgner et al., 1999b). For these pulse durations, KLM (Sec. 1.4.3) is required, and self-starting may be achieved with a SESAM in addition (Sutter et al., 1999). With a SESAM alone, 13 fs pulses with 80 mW have been demonstrated. If significantly longer pulse durations are acceptable, several watts of average power can be generated with a commercially available Ti^{3+}:sapphire laser, usually pumped with an argon ion laser. Recently, Cr^{2+}:ZnSe (Page et al., 1997) was identified as another very interesting gain material that is in various ways similar to Ti^{3+}:sapphire but emits at mid-infrared wavelengths, around 2.2–2.8 μm. This very broad bandwidth should allow for pulse durations below 20 fs, although to date the shortest achieved pulse duration is much longer, ≈ 4 ps (Carrig et al., 2000).

Diode-pumped femtosecond lasers can be built with crystals such as Cr^{3+}:LiSAF, Cr^{3+}:LiSGaF, or Cr^{3+}:LiSCAF, which can be pumped at longer wavelengths. However, these media have much poorer thermal properties and thus cannot compete with Ti^{3+}:sapphire in terms of output power. Cr^{3+}:LiSAF lasers have generated pulses as short as 12 fs (Uemura and Torizuka, 1999), but only with 23 mW of output power, using KLM without self-starting ability. The highest achieved modelocked power was 0.5 W in 110 fs pules (Kopf et al., 1997).

Cr^{4+}:forsterite emits around 1.3 μm and is suitable for pulse durations down to 14 fs with 80 mW (Chudoba et al., 2000), or 78 fs pulses with 800 mW (Petrov et al., 1998). Normally, an Nd-doped laser (which may be diode-pumped) is used for pumping of Cr^{4+}:forsterite. The same holds for Cr^{4+}:YAG, which emits around 1.4–1.5 μm and has allowed the generation of pulses of 43 fs duration at 200 mW (Tong et al., 1997).

Other broadband gain materials are phosphate or silicate glasses doped with rare earth ions such as Nd^{3+} or Yb^{3+}, for pulse durations down to ≈ 60 fs (Aus der Au et al., 1997; Hönninger et al., 1998) and output powers of a few hundred milliwatts. The relatively poor thermal properties make high-power operation challenging. Up to 1.4 W of average power in 275 fs pulses (Paschotta et al., 2000a) or 1 W in 175 fs pulses (Aus der Au et al., 1998) have been obtained from Nd^{3+}:glass by using a specially adapted elliptical mode pumping geometry (Paschotta et al., 2000b). Here, a strongly elliptical pump beam and laser mode allow the use of a fairly thin gain medium that can be efficiently cooled from both flat sides. The resulting nearly one-dimensional heat flow reduces the thermal lensing compared to cylindrical rod geometries if the aspect ration is large enough.

Yb^{3+}:YAG has thermal properties similar to those of Nd^{3+}:YAG and at the same time a much larger amplification bandwidth. Another favorable property is the small quantum defect. However, challenges arise from the quasi-three-level nature of this medium and from the small laser cross sections, which favor Q-switching instabilities. High pump intensities help in both respects. An end-pumped laser based on a Yb^{3+}:YAG rod has generated 340 fs pulses with 170 mW (Hönninger et al., 1995). As much as 8.1 W in 2.2 ps pulses was obtained from an elliptical mode Yb^{3+}:YAG laser (Aus der Au et al., 1999). Recently, the first Yb^{3+}:YAG thin disk laser (Giesen et al., 1994) was passively modelocked, generating 700 fs pulses with 16.2 W average power (Aus der Au et al., 2000). The concept of the passively modelocked thin disk laser appears to be power-scalable, so that even much higher powers should become possible in the near future.

A few Yb^{3+}-doped crystalline gain materials have been developed that combine a relatively broad amplification bandwidth (sufficient for pulse durations of a few hundred femtoseconds) with thermal properties that are better than those of other broadband materials, although not as good as, for example, those of YAG or sapphire. Examples are Yb^{3+}:YCOB (Valentine et al., 2000), Yb^{3+}:YGdCOB (Druon et al., 2000), Yb^{3+}:SFAP (Gloster et al., 1997), and Yb^{3+}:KGW (Brunner et al., 2000). With an end-pumped Yb^{3+}:KGW rod, 1.1 W of average power has recently been achieved in 176 fs pulses (Brunner et al., 2000). Yb^{3+}:KGW and Yb^{3+}:KYW may be applicable in a thin disk laser, possibly generating tens of watts in pulses with <200 fs duration, but this remains to be demonstrated. Another new class of materials of particular importance are the Yb^{3+}-doped sesquioxides (Larionov et al., 2001) such as Y_2O_3, Sc_2O_3, and Lu_2O_3, which appear to be very suitable for high-power operation.

Color center crystals can also be used for femtosecond pulse generation (Blow and Nelson, 1988; Yakymyshyn et al., 1989; Islam et al., 1989), but we do not discuss them here because they need cryogenic conditions.

1.3 DISPERSION AND NONLINEARITIES

1.3.1 Dispersion

When a pulse travels through a medium, it acquires a frequency-dependent phase shift. A phase shift that varies linearly with the frequency corresponds to a time delay, without any change of the temporal shape of the pulse. Higher order phase shifts, however, tends to modify the pulse shape and are thus of relevance for the formation of short pulses. The phase shift can be expanded in a Taylor series around the center angular frequency ω_0 of the pulse:

$$\varphi(\omega) = \varphi_0 + \frac{\partial\varphi}{\partial\varphi}(\omega-\omega_0) + \frac{1}{2}\frac{\partial^2\varphi}{\partial\omega^2}(\omega-\omega_0)^2 + \frac{1}{6}\frac{\partial^3\varphi}{\partial\omega^3}(\omega-\omega_0)^3 + \cdots \qquad (1)$$

Here the derivatives are evaluated at $\omega_0 \cdot \partial\varphi/\partial\omega$ is the group delay T_g, $\partial^2\varphi/\partial\omega^2$ the group delay dispersion (GDD), and, $\partial^3\varphi/\partial\omega^3$ the third-order dispersion (TOD). The GDD describes a linear frequency dependence of the group delay and thus tends to separate the frequency components of a pulse: For positive GDD, e.g., the components with higher frequencies are delayed with respect to those with lower frequencies, which results in a positive "chirp" ("up-chirp") of the pulse. Higher orders of dispersion generate more complicated distortions.

The broader the bandwidth of the pulse (i.e., the shorter the pulse duration), the more terms of this expansion are significant. GDD, which acts on an initially unchirped Gaussian pulse with full width at half maximum (FWHM) pulse duration τ_0, increases the pulse duration according to

$$\tau = \tau_0\left[1 + \left(4\ \ln\ 2\frac{\text{GDD}}{\tau_0^2}\right)^2\right]^{1/2} \qquad (2)$$

It is apparent that the effect of GDD becomes strong if $\text{GDD} > \tau_0^2$. Similarly, TOD becomes important if $\text{TOD} > \tau_0^3$.

1.3.2 Dispersion Compensation

If no dispersion compensation is used, the net GDD for one cavity round-trip is usually positive, mainly because of the dispersion in the gain medium.

Other components such as mirrors may also contribute to this. However, in lasers with $>10\,\mathrm{ps}$ pulse duration the dispersion effects can often be ignored, because the total GDD in the laser cavity is typically at most a few thousand square femtoseconds, much less than the pulse duration squared. For shorter pulse durations, the GDD has to be considered, and pulse durations below about 30 fs usually necessitate the compensation of TOD or even higher orders of dispersion. In most cases, the desired total GDD is not zero but negative, so that soliton formation (see Sec. 1.3.4) can be exploited. Usually, one requires sources of negative GDD and in addition appropriate higher order dispersion for shorter pulses. The most important techniques for dispersion compensation are discussed in the following subsections.

Dispersion from Wavelength-Dependent Refraction

If the intracavity laser beam hits a surface of a transparent medium with non-normal incidence, the wavelength dependence of the refractive index can cause wavelength-dependent refraction angles. In effect, different wavelength components will travel on slightly different paths, and this in general introduces an additional wavelength dependence to the round-trip phase and thus a contribution to the overall dispersion. The most frequently used application of this effect is to insert a prism pair in the cavity (Fork et al., 1984), where the different wavelength components travel in different directions after the first prism and along parallel but separated paths after the second prism. The wavelength components can be recombined simply on the way back after reflection at a plane end mirror (of a standing wave cavity) or by a second prism pair (in a ring cavity). Spatial separation of different wavelengths occurs only in part of the cavity. The negative GDD obtained from the geometric effect is proportional to the prism separation, and an additional (usually positive) GDD contribution results from the propagation in the prism material. The latter contribution can be easily adjusted via the prism insertion, so that the total GDD can be varied over an appreciable range. Some higher order dispersion is also generated, and the ratio of TOD and GDD can for a given prism material be varied only in a limited range by using different combinations of prism separation and insertion. Some prism materials with lower dispersion (e.g., fused quartz instead of SF10 glass) can help to reduce the amount of TOD generated together with a given value of GDD but also require greater prism separation. The prism angles are usually not used as optimization parameters but rather are set to be near Brewster's angle in order to minimize reflection losses. The small losses and the versatility of the prism pair technique are the reasons prism pairs are very widely used in ultrafast lasers.

In Ti^{3+}:sapphire lasers, pulse durations around 10 fs can be reached with negative dispersion only from a prism pair.

More compact geometries for dispersion compensation make use of a single prism only (Ramaswamy-Paye and Fujimoto, 1994; Kopf et al., 1996b). In this case, the wavelength components are spatially separated in the whole resonator, not just part of it. Even without any additional prisms, refraction at a Brewster interface of the gain medium can generate negative dispersion. In certain configurations, where the cavity is operated near a stability limit, the refraction effect can be strongly increased (Paschotta et al., 1999a), so significant negative GDD can be generated in a compact cavity. The amount of GDD may then also strongly depend on the thermal lens in the gain medium and on certain cavity dimensions.

Grating Pairs

Compared to prism pairs, pairs of diffraction gratings can generate higher dispersion in a compact setup. However, because of the limited diffraction efficiency of gratings, the losses of a grating pair are typically higher than acceptable for use in a laser cavity, except in cases with a high gain (e.g., in fiber lasers). For this reason, grating pairs are normally used only for external pulse compression.

Gires-Tournois Interferometers (GTIs)

A compact device to generate negative GDD (even in large amounts) is the Gires-Tournois interferometer (GTI) (Gires and Tournois, 1964), which is a Fabry-Perot interferometer operated in reflection. Because the rear mirror is highly reflective, the GTI as a whole is highly reflective over the whole wavelength range, whereas the phase shift varies nonlinearly by 2π for each free spectral range, calculated as $\Delta\nu = c/2nd$, where n and d are refractive index and the thickness of the spacer material, respectively. Within each free spectral range, the GDD oscillates between two extremes the magnitude of which is proportional to d^2 and also depends on the front mirror reflectivity. Ideally, the GTI is operated near a minimum of the GDD, and the usable bandwidth is some fraction (e.g., one-tenth) of the free spectral range, which is proportional to d^{-1}. Tunable GDD can be achieved if the spacer material is a variable air gap, which, however, must be carefully stabilized to avoid unwanted drifts. More stable but not tunable GDD can be generated with monolithic designs, based, e.g., on thin films of dielectric media such as TiO_2 and SiO_2, particularly for use in femtosecond lasers. The main drawbacks of GTI are the fundamentally limited bandwidth (for a given amount of GDD) and the limited amount of control of higher order dispersion.

Dispersive Mirrors

Dielectric Bragg mirrors with regular $\lambda/4$ stacks have a fairly small dispersion when operated well within their reflection bandwidth, but increasing dispersion at the edges of this range. Modified designs can be used to obtain well-controlled dispersion over a large wavelength range. One possibility already discussed is the use of a GTI structure (see preceding subsection). Another broad range of designs are based on the concept of the chirped mirror: If the Bragg wavelength is appropriately varied within a Bragg mirror design, longer wavelengths can be reflected deeper in the structure, thus acquiring a larger phase change, which leads to negative dispersion. However, the straightforward implementation of this idea leads to strong oscillations of the GDD (as a function of frequency), which render such designs useless. These oscillations can be greatly reduced by numerical optimizations that introduce complicated (and not analytically explainable) deviations from the simple chirp law. A great difficulty is that the figure of merit to optimize is a complicated function of many layer thickness variables; it typically has a large number of local extremes and thus is quite difficult to optimize. Nevertheless, refined computing algorithms led to designs with respectable performance that were realized with precision growth of dielectric mirrors. Such mirrors can compensate for the dispersion in Ti^{3+}:sapphire lasers for operation with pulse durations well below 10 fs (Jung et al., 1997). Further analytical studies led to the design of double-chirped mirrors, where both the Bragg wavelength and the coupling strength (determined by the ratio of thickness for low- and high-index layers) are varied, and a broadband high quality antireflection coating on the front surface is used in addition (Kärtner et al., 1997). Because such analytically found designs are already close to optimum, a slight refinement by local numerical optimization is sufficient to arrive at very broadband designs. Mirrors based on such designs have been used in Ti^{3+}:sapphire lasers to generate pulses with durations of <6 fs (Morgner et al., 1999b; Sutter et al., 2000), which are the shortest pulses ever generated directly from a laser.

Dispersive SESAMs

Negative dispersion can also be obtained from semiconductor saturable absorber mirrors (SESAMs) (see Sec. 1.4.3) with specially modified designs. The simplest option is to use a GTI-like structure (see earlier in this section) (Kopf et al., 1996a). A double-chirped dispersive semiconductor mirror has also been demonstrated (Paschotta et al., 1999b), and a saturable absorber could be integrated into such a device.

1.3.3 Kerr Nonlinearity

Because of the high intracavity intensities, the Kerr effect is relevant in most ultrafast lasers. The refractive index. of, e.g., the gain medium is modified according to

$$n(I) = n_0 + n_2 I \tag{3}$$

where I is the laser intensity and n_2 a material-dependent coefficient that also weakly depends on the wavelengths. (The pump intensity is normally ignored because it is far smaller than the peak laser intensity.) These nonlinear refractive index changes have basically two consequences. The first is a transverse index gradient resulting from the higher intensities on the beam axis compared to the intensities in the wings of the transverse beam profile. This leads to a so-called Kerr lens with an intensity-dependent focusing effect (for positive n_2) that can be exploited for a passive modelocking mechanism as discussed in Section 1.4.3.

The second consequence of the Kerr effect is that the pulses experience self-phase modulation (SPM): The pulse center is delayed more (for positive n_2) than the temporal wings. For a freely propagating Gaussian transverse beam profile of radius w (defined so that at this radius we have $1/e^2$ times the peak intensity), the nonlinear coefficient γ_{SPM}, related the on-axis phase change φ to the pulse power P according to $\varphi = \gamma_{\mathrm{SPM}} P$, is given by

$$\gamma_{\mathrm{SPM}} = \frac{2\pi}{\lambda} n_2 \left(\frac{\pi w^2}{2}\right)^{-1} L = \frac{4 n_2 L}{\lambda w^2} \tag{4}$$

where L is the propagation length in the medium. Note that the peak intensity of a Gaussian beam is $I = P/(\pi w^2/2)$, and the on-axis phase change (and not an averaged phase change) is relevant for freely propagating beams. For guided beams, an averaged phase change has to be used, which is two times smaller.

The most important consequences of SPM in the context of ultrafast lasers is the possibility of soliton formation (Sec. 1.3.4). Another important aspect is that SPM can increase or decrease the bandwidth of a pulse, depending on the original phase profile of the pulse. In general, positive SPM tends to increase the bandwidth of positively chirped (i.e., up-chirped) pulses, whereas negatively chirped pulses can be spectrally compressed. An originally unchirped pulse traveling through a nonlinear a nondispersive medium will experience an increase of bandwidth only to second order of the propagation distance, whereas a chirp grows in first order.

1.3.4 Soliton Formation

If a pulse propagates through a medium with both second-order dispersion (GDD) and a Kerr nonlinearity, the two effects can interact in complicated ways. A special case is that the intensity has a sech^2 temporal profile

$$P(t) = P_p \,\mathrm{sech}^2\left(\frac{t}{\tau_S}\right) = \frac{P_p}{\cosh^2(t/\tau_S)} \tag{5}$$

with the peak power P_p and the FWHM pulse duration $\tau_{\mathrm{FWHM}} \approx 1.76\tau_S$. If such a pulse is unchirped and fulfills the condition

$$\tau_S = \frac{2|\mathrm{GDD}|}{|\gamma_{\mathrm{SPM}}| E_p} \tag{6}$$

where GDD and γ_{SPM} have opposite signs and are calculated for the same propagation distance, and

$$E_p \approx 1.13 P_p \tau_{\mathrm{FWHM}} \tag{7}$$

is the pulse energy, then we have a so-called fundamental soliton. Such a pulse propagates in the medium with constant temporal and spectral shape and acquires only an overall nonlinear phase shift. Higher order solitons, where the peak power is higher by a factor that is the square of an integral number, do not preserve their temporal and spectral shape but evolve in such a way that the original shape is restored after a certain propagation distance, the so-called soliton period in the case of a second-order soliton.

Solitons are remarkably stable against various kinds of distortions. In particular, stable soliton-like pulses can be formed in a laser cavity even though dispersion and Kerr nonlinearity occur in discrete amounts and the pulse energy varies due to amplification in the gain medium and loss in other elements. As long as the soliton period amounts to many (at least about five to ten) cavity round-trips, the solition simply "sees" the average GDD and Kerr nonlinearity, and this "average solition" behaves in the same way as in a homogeneous medium. The soliton period in terms of the number of cavity round-trips is

$$N_S = \frac{\pi\tau_S^2}{2|\mathrm{GDD}|} \approx \frac{\tau_{\mathrm{FWHM}}^2}{2|\mathrm{GDD}|} \tag{8}$$

where GDD is calculated for one cavity round-trip. N_S is typically quite large in lasers with pulse durations of $> 100\,\mathrm{fs}$, so the average soliton is a good approximation. Once N_S becomes less than about 10, the soliton is significantly disturbed by the changes of dispersion and nonlinearity during a round-trip, and this may lead to pulse break-up. In Ti^{3+}:sapphire lasers for pulse durations below 10 fs, the regime of small N_S is unavoidable and can be stabilized only by using a fairly strong saturable absorber. On the other hand, in cases with very large values of N_S it can be beneficial to decrease N_S by increasing both |GDD| and γ_{SPM}, because stronger soliton shaping can stabilize the pulse shape and spectrum and make the pulse less dependent on other influences.

Note that soliton effects can fix the pulse duration at a certain value even if other cavity elements (most frequently the laser gain with its limited bandwidth) tend to reduce the pulse bandwidth. The pulse will then acquire a positive chirp (assuming $n_2 > 0$ for the Kerr medium), and under these conditions SPM can generate the required extra bandwidth.

1.4 MODELOCKING

1.4.1 General Remarks

Ultrashort light pulses are in most cases generated by modelocked lasers. In this regime of operation, usually a single short pulse propagates in the laser cavity and generates an output pulse each time it hits the output coupler mirror. The generated pulses are usually quite short compared to the round-trip time.

In the frequency domain, modelocking means operation of the laser on a number of axial cavity modes, whereby all these modes oscillate in phase (or at least with nearly equal phases). In this case, the mode amplitudes interfere constructively only at certain times, which occur with the period of the round-trip time of the cavity. At other times, the output power is negligibly small. The term "modelocking" resulted from the observation that a fixed phase relationship between the modes has to be maintained in some way to produce short pulses. The achievable pulse duration is then inversely proportional to the locked bandwidth, i.e., to the number of locked modes time their frequency spacing.

It is obvious in the domain description that modelocking cannot be achieved if a significant amount of the laser power is contained in higher order transverse modes of the cavity, because these usually have different resonance frequencies, so that the periodic recurrence of constructive addition of all mode amplitudes is not possible. Therefore, laser operation on the fundamental transverse cavity mode (TEM_{00}) is usually a prerequisite to stable modelocking.

In some cases, a modelocked laser is operated with several pulses circulating in the cavity. This mode of operation, called "harmonic mode-locking," can be attractive for the generation of pulse trains with higher repetition rates. The main difficulty is that the timing between the pulses has to be maintained in some way, either by some kind of interaction between the pulses or with the aid of externally applied timing information. A number of solutions have been found, but in this chapter we concentrate on fundamental modelocking, with a single pulse in the laser cavity, as it occurs in most ultrafast lasers.

So far we have assumed that the modelocked laser operates in a steady state, where the pulse energy and duration may change during a round-trip (as an effect of gain and loss, dispersion, nonlinearity, etc.) but always return to the same values at a certain position in the cavity. This regime is called cw (continuous-wave) modelocking and is indeed very similar to ordinary cw (not modelocked) operation, because the output power in each axial cavity mode is constant over time. Another important regime is Q-switched modelocking (Sec. 1.4.3), where the modelocked pulses are contained in periodically recurring bunches that have the envelope of a Q-switched pulse. It is in some cases a challenge to suppress an unwanted tendency for Q-switched modelocking.

In addition to Q-switching tendencies, a number of other mechanisms can destabilize the modelocking behavior of a laser. In particular, short pulses have a broader bandwidth than, e.g., a competing cw signal and thus tend to experience less gain than the latter. For the pulses to be stable, some mechanism is required that increases the cavity loss for cw signals more than for pulses. Also, a modelocking mechanism should ideally give a clear loss advantage for shorter pulses compared to any other mode of operation. We discuss various stability criteria in the following sections.

Mechanisms for modelocking are grouped into active and passive schemes and hybrid schemes that utilize a combination of the two. Active modelocking (Sec. 1.4.2) is achieved with an active element (usually an acousto-optic modulator) generating a loss modulation that is precisely synchronized with the cavity round-trips. Passive schemes (Sec. 1.4.3) rely on a passive loss modulation in some type of saturable absorber. This passive loss modulation can occur on a much faster time scale, so that passive modelocking typically allows for the generation of much shorter pulses. Passive schemes are also usually simpler, because they do not rely on driving circuits and synchronization electronics. The pulse timing is then usually not externally controlled. Synchronization of several lasers is more easily achieved with active modelocking schemes.

Modelocked lasers are in most cases optically pumped with a cw source, e.g., one or more laser diodes. This requires a gain medium that can store the excitation energy over a time of more than one cavity round-trip (which typically takes a few nanoseconds). Typical solid-state gain materials fulfill this condition very well, even for rather low repetition rates, because the lifetime of the upper laser level is usually at least a few microseconds, in some cases even more than a millisecond. Synchronous pumping (with a modelocked source), as is often used for dye lasers, is therefore rarely applied to solid-state lasers and is not discussed in this chapter.

In the following sections we discuss some details of active and passive modelocking. The main emphasis is on passive modelocking, because such techniques clearly dominate in ultrafast optics.

1.4.2 Active Modelocking

An actively modelocked laser contains some kind of electrically controlled modulator, in most cases of acousto-optic and sometimes of electro-optic type. The former uses a standing acoustic wave with a frequency of tens or hundreds of megahertz, generated with a piezoelectric transducer in an acousto-optic medium. In this way one obtains a periodically modulated refractive index pattern at which the laser light can be refracted. The refracted beam is normally eliminated from the cavity, and the refraction loss oscillates with twice the frequency of the acoustic wave because the refractive index change depends only on the modulus of the pressure deviation.

A pulse circulating in the laser cavity is hardly affected by the modulator provided that it always arrives at those times when the modulator loss is at its minimum. Even then, the temporal wings of the pulse experience a somewhat higher loss than the pulse center. This mechanism tends to shorten the pulses. On the other hand, the limited gain bandwidth always tends to reduce the pulse bandwidth and thus to increase the pulse duration. Other effects such as dispersion or self-phase modulation (Sec. 1.3) can have additional influences on the pulse. Usually, a steady state is reached where the mentioned competing effects exactly cancel each other for every complete cavity round-trip.

The theory of Kuizenga and Siegman (Kuizenga and Siegman, 1970) describes the simplest situation with a modulator (in exact synchronism with the cavity) and gain filtering but no dispersion or self-phase modulation. The gain is assumed to be homogeneously broadened and of Lorentzian shape. The simple result is the steady-state FWHM pulse duration

$$\tau \approx 0.45\left(\frac{g}{M}\right)^{1/4}(f_m\ \Delta f_g)^{-1/2} \tag{9}$$

where g is the power gain at the center frequency, M is the modulation strength ($2M$ = peak-to-peak variation of power transmission), f_m is the modulation frequency, and Δf_g is the FWHM gain bandwidth. The peak gain g is slightly higher than the cavity loss l (for minimum modulator loss) according to

$$g = l + \frac{M}{4}(2\pi f_m \tau)^2 \tag{10}$$

so that the total cavity losses (including the modulator losses) are exactly balanced for the pulse train. Note that the losses would be higher than the gain for either a longer pulse (with higher modulator loss) or a shorter pulse (with stronger effect of gain filtering).

It is important to note that for non-Lorentzian gain spectra the quantity Δf_g should be defined such that the corresponding Lorentzian reasonably fits the gain spectrum within the pulse bandwidth, which may be only a small fraction of the gain bandwidth; only the "curvature" of the gain spectrum within the pulse bandwidth is important. This means that even weak additional filter effects, caused, e.g., by intracavity reflections (etalon effects), can significantly reduce the effective bandwidth and thus lead to longer pulses. Such effects are usually eliminated by avoiding any optical interfaces that are perpendicular to the incident beam. Also note that the saturation of inhomogeneously broadened gain can distort the gain spectrum and thus affect the pulse duration.

With SPM in addition (but no dispersion), somewhat shorter pulses can be generated, because SPM can generate additional bandwidth. However, with too much SPM the pulses become unstable. It has been shown with numerical simulations (Haus et al., 1991) that a reduction of the pulse duration by a factor on the order of 2 is possible. The resulting pulses are then chirped, so that some further compression with extracavity negative dispersion is possible.

The situation is quite different if positive SPM occurs together with negative GDD, because in this case soliton-like pulses (Sec. 1.3.4) can be formed. If the soliton length corresponds to at least about 10 but less than 100 cavity round-trips, soliton-shaping effects can be much stronger than the pulse-shaping effect of the modulator. The pulse duration is then determined only by the soliton equation, Eq. (6). The solition experiences only a very small loss at the modulator. However, owing to its bandwidth it also experiences less gain than, e.g., a long background pulse, the so-called continuum, which can have a small bandwidth. The shorter the soliton pulse duration, the smaller the soliton gain compared to the continuum gain and the higher the modulator strength M must be to keep the soliton stable against growth of the continuum. Using results from Kärtner et al. (1995a), it can be shown that the minimum pulse duration is proportional to

$$\frac{g^{1/3}}{\Delta f_g^{2/3}} \left(\frac{N_S}{M}\right)^{1/6} \tag{11}$$

where N_S is the soliton period in terms of cavity round-trips. This indeed shows that a smaller modulator strength is sufficient if N_S is kept small, but also that the cavity loss should be kept small (to keep g small) and the gain bandwidth is the most important factor.

With gain media like Nd^{3+}:YAG or Nd^{3+}:YLF, typical pulse durations of actively modelocked lasers are a few tens of picoseconds. The minimum appears to be 6.2 ps (Walker et al., 1990). Using Nd^{3+}:glass and the regime of soliton formation, pulse durations of around 7 ps have been achieved (Yan et al., 1986). For significantly shorter pulses, active modelocking is not effective because the time window of low modulator loss would be much longer than the pulse duration.

1.4.3 Passive Modelocking

The Starting Mechanism

Passive modelocking relies on the use of some type of saturable absorber, which favors the generation of a train of short pulses against other modes of operation such as cw emission. Starting from a cw regime, the saturable absorber will favor any small noise spikes, so those can grow faster than the cw background. Once these noise spikes contain a significant part of the circulating energy, they saturate the gain so that the cw background starts to decay. Later on, the most energetic noise spike, which experiences the least amount of saturable absorption, will eliminate all the others by saturating the gain to a level where these experience net loss in each round-trip. In effect we obtain a single circulating pulse. Owing to the action of the saturable absorber, which favors the peak over the wings of the pulse, the duration of the pulse is then reduced further in each cavity round-trip, until broadening effects (e.g., dispersion) become strong enough to prohibit further pulse shortening. Note that other shortening effects, e.g., soliton-shaping effects, can also become effective.

The described start-up can be prevented if strong pulse-broadening effects are present in an early phase. In particular, the presence of spurious intracavity reflections can be significant, because those tend to broaden (or split up) pulses even before they have acquired a significant bandwidth. A significantly stronger saturable absorber may then be required to get self-starting modelocking. These effects are usually difficult to quantify but can be suppressed in most bulk solid-state lasers by using suitable designs. For example, even antireflection-coated surfaces in the cavity should be slightly tilted against the laser beam so that beams resulting from residual reflections are eliminated from the cavity.

Note that a saturable absorber with long recovery time (low saturation intensity) is most effective for fast self-starting modelocking, although a short recovery time may allow the generation of shorter pulses. Other techniques to facilitate self-starting modelocking include the use of optical feedback from a moving mirror (Smith, 1967), which tends to increase the intracavity fluctuations in cw operation.

Parameters of Fast and Slow Saturable Absorbers

An important parameter of a saturable absorber is its recovery time. In the simplest case, we have a so-called fast saturable absorber, which can recover on a faster time scale than the pulse duration. In this case the state of the absorber is largely determined by the instantaneous pulse intensity, and strong shaping of the leading edge as well as the trailing edge of the pulse takes place. However, for short enough pulse durations we have the opposite situation of a slow absorber, with the absorber recovery occurring on a long time scale compared to the pulse duration. This regime is frequently used in ultrafast lasers, because the choice of fast saturable absorbers is very limited for pulse durations below 100 fs. We discuss in the following subsection why it is possible that pulses with durations well below 100 fs can be generated even with absorbers that are much slower.

Concrete types of saturable absorbers are compared in the following subsection. Here we discuss some parameters that can be used to quantitatively characterize the action of saturable absorbers.

The intensity loss* q generated by a fast saturable absorber depends only on the instantaneous intensity I, the incident power divided by the mode area. Simple absorber models lead to a function

$$q(I) = \frac{q_0}{1 + I/I_{\text{sat}}} \tag{12}$$

which is a reasonable approximation in many cases. The response is then characterized by the parameter I_{sat}, called the saturation intensity, and the unsaturated loss q_0. For pulses with a given peak intensity I_p, an average value of q can be calculated that represents the effective loss for the pulse. Figure 2 shows this quantity as a function of the normalized peak intensity for Gaussian and solition (sech^2) pulses, together with $q(I_p)$. We see that the pulse form has little influence on the average loss.

The behavior of a slow saturable absorber is described by the differential equation

*Note that some authors define q as the amplitude (instead of intensity) loss coefficient, which is one-half the value used here.

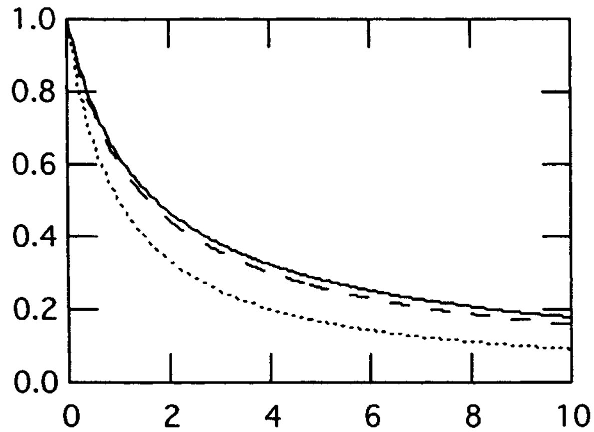

Figure 2 Solid curve: Effective loss for a soliton pulse on a fast saturable absorber, as a function of the ratio of peak intensity to the saturation intensity. Dashed curve: Same as for a Gaussian pulse. Dotted curve: Loss for the peak intensity.

$$\frac{dq}{dt} = -\frac{q - q_0}{\tau} - \frac{I}{F_{\text{sat}}} q \tag{13}$$

with the recovery time τ, the unsaturated loss q_0, and the saturation fluence F_{sat}. If the recovery is so slow that we can ignore the first term, then the value of q after a pulse with fluence F_{sat} is $q_0 \exp(-F_p/F_{\text{sat}})$ if the pulse hits an initially unsaturated absorber. The effective loss for the pulse is (independent of the pulse form)

$$q_p(F_p) = q_0 \left[1 - \exp\left(\frac{-F_p}{F_{\text{sat}}}\right)\right] \left(\frac{F_{\text{sat}}}{F_p}\right) = q_0 \frac{1 - \exp(-S)}{S} \tag{14}$$

with the saturation parameter $S := F_p/F_{\text{sat}}$. For strong saturation (as usual in modelocked lasers) ($S > 3$), the absorbed pulse fluence is $\approx F_{\text{sat}} \Delta R$, and we have

$$q_p(F_p) \approx q_0/S \tag{15}$$

Figure 3 shows a plot of this function, compared to the loss after the pulse. It is important to observe that the loss after the pulse gets very small for $S > 3$, whereas the average loss q_p for the pulse is still significant then.

Another important parameter for any saturable absorber is the damage threshold in terms of the applicable pulse fluence or intensity. Note that the absolute value of the damage threshold is actually less relevant than the ratio of the damage fluence and the saturation fluence, because the latter determines the typical operating parameters.

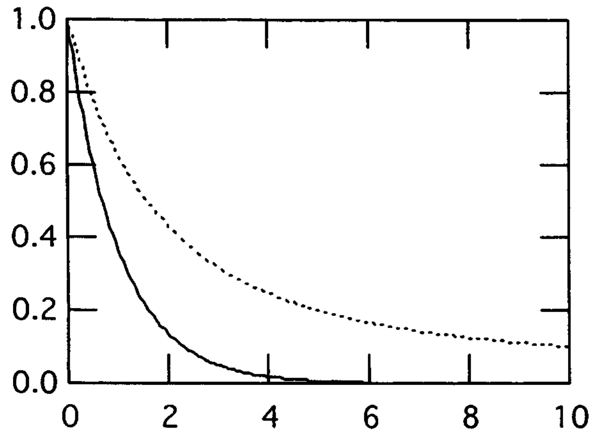

Figure 3 Dotted curve: Loss for a pulse on a slow saturable absorber, as a function of the saturation parameter (pulse energy divided by saturation energy). Solid curve: Loss after the pulse.

Passive Modelocking with Fast and Slow Saturable Absorbers

Here we give some guidelines as to what pulse durations can be expected from passively modelocked lasers. First we consider cases with a fast saturable absorber and without significant influence of dispersion and self-phase modulation. We also assume that significant gain saturation does not occur during a pulse. For this situation, which can occur particularly in picosecond solid-state lasers modelocked with SESAMs (see later), analytical results have been obtained (Haus et al., 1991). These calculations are strictly valid only for weak absorber saturation, which is not the desired case, but numerical simulations show that for a fully saturated absorber the obtained pulse duration can be estimated from

$$\tau \approx \frac{0.9}{\Delta f_g}\sqrt{\frac{g}{\Delta R}} \tag{16}$$

where Δf_g is th FWHM gain bandwidth (assuming that a Lorentzian shape fits the gain spectrum well within the range of the pulse spectrum; see Sec. 1.4.2), g is the power gain coefficient (which equals the overall cavity losses), and ΔR is the modulation depth (maximum reflectivity change) of the absorber. Compared to the equation from the analytical results, we have increased the constant factor by about 10% because the analytical calculations are not accurate for a fully saturated gain and numerical simulations (which do not need to approximate the gain saturation with a linear function) result in typically $\approx 10\%$ longer pulse durations. Note that significantly weaker or stronger absorber saturation results in longer pulses. If we introduce some self-phase modulation, the pulse duration can be somewhat reduced because this effect helps to increase the pulse bandwidth. However, the dynamics become unstable if too much self-phase modulation occurs. The same holds for phase changes that can arise in an absorber when it is saturated.

Note that an increase in ΔR also increases the required gain g, so that a value of ΔR greater than the linear cavity losses does not significantly reduce the pulse duration. The limit for the pulse duration is on the order of $1/\Delta f_g$.

With a slow saturable absorber, somewhat longer pulse durations are obtained. Without significant influence of dispersion and self-phase modulation, we can estimate the pulse duration (Paschotta and Keller, 2001) with

$$\tau \approx \frac{1.07}{\Delta f_g}\sqrt{\frac{g}{\Delta R}} \tag{17}$$

This equation, which is very similar to Eq. (16), is an empirical fit to results from numerical simulations. It holds if the absorber is operated at roughly 3–5 times the saturation fluence. For significantly weaker or stronger absorber saturation, the pulse duration gets somewhat longer. In contrast to the situation for fast absorbers, the influence of self-phase modulation always makes the pulses longer, apart from the instability occurring when the effect is too strong. Particularly in femtosecond lasers, it can be difficult to make the nonlinearity weak enough. In this case, soliton mode locking (see below) is a good solution. Here, a significant nonlinear phase shift is even desirable for good stability.

The pulse duration obtained with a slow saturable absorber can be significantly shorter than the absorber recovery time; but in such cases the stability and pulse quality can be somewhat reduced because a weak pedestal can grow behind the pulse. This result may seem quite surprising because a slow absorber can clean up only the leading part of the pulse, not the trailing part. However, only a little energy can be fed into the trailing part as long as dispersion effects are weak. Also, the pulse is constantly delayed because the absorber attenuates the leading part; in effect, the pulse tends to "eat up" the trailing part, which is not delayed (Paschotta and Keller, 2001).

In the femtosecond regime, many absorbers (including SESAMs) become slow compared to the pulse duration. The question arises as to how stable modelocked operation can be achieved with a pulse duration much shorter than the absorber recovery time. In dye lasers, it was found that gain saturation during each pulse can very much shorten the time window with effective gain: After the passage of the pulse, the absorber stays saturated for a while, but the gain is also exhausted and may need some longer time to recover. For this reason, dye lasers can be used to generate pulses with durations down to ≈ 27 fs (Valdmanis et al., 1985) [with external compression, even 6 fs (Fork et al., 1987)], which is much less than the absorber recovery time (typically on the order of 0.1 ns to a few nanoseconds for dye absorbers). In ion-doped solid-state gain media, this principle cannot be used because such gain media have relatively small laser cross sections, and the gain saturation fluence is much larger than the achievable pulse fluence. Therefore, gain saturation occurs only on a time scale on the order of the fluorescence decay time and is caused by the integral effect of many pulses, whereas gain saturation by a single pulse is very weak. Nevertheless it has been shown that even from solid-state media one can obtain pulses that are much shorter than the absorber recovery time. This is particularly the case if the mechanism of soliton modelocking (Kärtner and Keller, 1995) is employed. In the regime of negative intracavity dispersion, soliton effects (see Sec. 1.3.4) can fix the pulse duration at a certain value. The saturable absorber is then required only to start the modelocking process and to stabilize the solitons. The latter means that two types of instability must be suppressed. First, a competing cw background (or long pulse pedestal) can have less bandwidth and thus experience more gain than the soliton, but this can be suppressed by the saturable absorber because this introduces a higher loss for the background. Second, pulse breakup could occur because a breakup into two solitons with, e.g., half the energy would increase the gain (because of the reduced pulse bandwidth); the absorber must prevent this by having a higher loss for two pulses compared to the single pulse. It turns out that the limit for the pulse duration depends only weakly on the modulation depth and recovery time of the absorber.

Note that apart from the shortest achievable pulse duration, self-starting modelocking is also a desirable goal. In this respect, a slow absorber is usually superior, because it has a lower saturation intensity, which facilitates the modelocking process in an early phase, as discussed earlier in this section.

Saturable Absorbers for Passive Modelocking

In this section we discuss a number of different saturable absorbers (or artificial saturable absorbers) for passive modelocking, concentrating on the most important techniques for ultrashort-pulse generation.

Semiconductor Absorbers. A semiconductor can absorb light if the photon energy is sufficient to excite carriers from the valence band to the conduction band. Under conditions of strong excitation, the absorption is saturated because possible initial states of the pump transition are depleted while the final states are partially occupied. Within typically 60–300 fs after the excitation, the carriers in each band thermalize, and this leads to a partial recovery of the absorption. On a longer time scale—typically between a few picoseconds and a few nanoseconds—they will be removed by recombination and trapping. Both processes can be used for modelocking of lasers.

A few percent of the incident radiation can be absorbed in a semiconductor layer of only a few nanometers thickness. Such a structure is called a quantum well because for structures with such small dimensions the density of states is modified by quantum effects. Quantum well absorbers or somewhat thicker absorbers (called bulk absorbers) are usually integrated into a microstructure with different surrounding semiconductor materials that are not absorbing due to a larger band gap. Typically, such structures are grown on a semiconductor wafer ≈ 0.5 mm thick (of GaAs, e.g.) and contain a Bragg mirror structure so they can be operated in reflection. In some cases, the Bragg mirror is replaced by a metallic mirror with broader bandwidth (Jung et al., 1997). In any case, such a structure has been called a semiconductor saturable absorber mirror (SESAM) since its first use for modelocking in 1992 (Keller et al., 1992). This acronym includes all types of saturable semiconductor absorbers that are operated in reflection. Most SESAMs contain a Bragg mirror, and if the absorber is incorporated into the top part of this Bragg mirror, the term saturable Bragg reflector (SBR) introduced in 1995 (Tsuda et al., 1995), is also sometimes used.

Most SESAMs that are used nowadays consist of a semiconductor Bragg mirror and a quantum well or bulk absorber, usually embedded between two nonabsorbing semiconductor layers grown on top of this mirror. The semiconductor air interface has a reflectivity of $\approx 30\%$, which together with the Bragg mirror forms a Fabry-Perot structure. In most cases, the SESAM is designed so that this Fabry-Perot is antiresonant at the operation wavelengths. In this regime, the largest possible bandwidth is achieved, and the saturation fluence is on the order of $100\,\mu\text{J/cm}^2$. (The absorber layer itself would have a saturation fluence on the order of $30\,\mu\text{J/cm}^2$.) We call such a device a low-finesse SESAM. A higher finesse of the Fabry-Perot can be obtained with a dielectric top mirror. Such devices were initially used for modelocking of lasers (Keller et al., 1992) and were termed antiresonant Fabry-Perot saturable absorbers (A-FPSAs). Compared to the same SESAM without a top reflector, the high-finesse SESAM has a greater saturation fluence ($> 100\,\mu\text{J/cm}^2$) and an accordingly smaller modulation depth (which can often be compensated for with a thicker absorber layer, if required). The increased damage fluence is no advantage because such samples have to be operated at accordingly higher fluence values. For use in high-power lasers, low-finesse SESAMs operated with an accordingly larger laser spot size and lower pulse fluence are preferable (Paschotta et al., 2000a) because the generated heat is distributed over a larger area.

Most modelocked lasers are operated in wavelength regimes of around 0.71–0.9 μm (e.g., Ti^{3+}:sapphire) and 1.03–1.07 μm (e.g., Nd^{3+}:YAG, Nd^{3+}:glass, Yb^{3+}:YAG). For 0.8 μm, GaAs absorbers can be used together with Bragg mirrors made of AlAs and $Ga_xAl_{1-x}As$ (where the gadolinium content x is kept low enough to avoid absorption). For wavelengths around 1.03–1.064 μm, the Bragg mirrors can be made of GaAs and AlAs, and the absorber is made of $In_xGa_{1-x}As$, where the indium content x is adjusted to obtain a small enough band gap. Because $In_xGa_{1-x}As$ cannot be grown lattice-matched to GaAs, increasing the indium content leads to increasing strain, which can lead to surface degradation by cracking and thus limits the absorber thickness. Nevertheless, such samples have been applied for modelocking of lasers operating around 1.3 μm (Fluck et al., 1996) and even 1.5 μm (Spühler et al., 1999a). SESAMs for 1.3 and 1.5 μm have also been developed on the basis of InGaAsP grown on InP substrates.

SEASAMs can be produced either with molecular beam epitaxy (MBE) or with metal-organic chemical vapor deposition (MOCVD). The MOCVD process is faster and thus appears to be most suitable for mass production. It also leads to relatively small nonsaturable losses, so that such SESAMs are well suited for high-power operation. Similarly low losses can be achieved with MBE. However, MBE gives us the additional flexibility to grow semiconductors at lower temperatures, down to $\approx 200°C$, whereas MOCVD is usually done at $\approx 600°C$. Lower growth temperatures lead to microscopic structural defects that act as traps for excited carriers and thus reduce the recovery time, which can be beneficial for use in ultrafast lasers. However, the nonsaturable losses of such samples also increase with decreasing growth temperature. This compromise between speed of recovery and quality of the surfaces can be improved by optimized annealing procedures or by beryllium doping (Haiml et al., 1999a, 1999b).

The presence of two different time scales in the SESAM recovery, resulting from intraband thermalization and carrier trapping and/or recombination, can be rather useful for modelocking. The longer time constant results in a reduced saturation intensity for part of the absorption, which facilitates self-starting modelocking, whereas the faster time constant is more effective in shaping subpicosecond pulses. Therefore, SESAMs make it possible to easily obtain self-starting modelocking in most cases.

SESAMs are quite robust devices. The ratio of the damage fluence to the saturation fluence is typically on the order of 100, so that a long device lifetime can be achieved with the usual parameters of operation (pulse fluence ≈ 3–10 times the saturation fluence). For high-power operation, the thermal load can be substantial, but the relatively good heat conductivity, e.g., of GaAs and the geometry of a thin disk allow for efficient cooling through the back side, which is usually soldered to a copper heat sink. The latter may be water-cooled in multiwatt lasers. Once the mode diameter is larger than the substrate thickness (typically 0.5 mm), further power scaling by increasing the mode area and keeping the pulse fluence constant will not substantially increase the temperature rise (Paschotta et al., 2000a). The temperature rise can be limited to below 100 K by the use of SESAM designs with low saturation fluence ($100\,\mu J/cm^2$ or less), because these allow operation with a larger mode area. SESAM damage can thus be avoided by using suitable designs and operation parameters, and further power scaling is not prohibited by such issues.

Recently, a new type of semiconductor-based saturable absorber, based on InAs semiconductor nanoparticles in silica, was demonstrated (Bilinsky et al., 1999a, 1999b). The fabrication technique may be well suitable for cheap mass production. Using such an absorber, modelocking of a Ti^{3+}:sapphire laser with 25 fs pulse duration was obtained. A disadvantage of these absorber devices is their high saturation fluence ($25\,mJ/cm^2$), at least about two orders of magnitude higher than for typical SESAMs. For this reason, strong focusing on the absorber is necessary, and high powers can probably not be handled.

Kerr Lens Modelocking. Very fast effective saturable absorbers, suitable for the generation of pulses with durations below 10 fs, can be implemented using the Kerr effect. In typical gain media, the Kerr effect (i.e., the dependence of the refractive index on the light intensity) has a time constant on the order of at most a few femtoseconds. The intensity gradients across the transverse mode profile, e.g., in the gain medium lead to a Kerr lens with intensity-dependent focusing power. This can be combined with an aperture to obtain an effective saturable absorber, which can be used for Kerr lens modelocking (KLM) (Keller et al., 1991; Negus et al., 1991; Salin et al., 1991). For example, a pinhole at a suitable location in the laser cavity leads to significant losses for cw operation but reduced losses for short pulses for which the beam radius at the location of the pinhole is reduced by the Kerr lens. This is called hard aperture KLM. Another possibility [soft aperture KLM (Piché et al., 1993)] is to use a pump beam that has a significantly smaller beam radius than the laser beam in the gain medium. In this situation, the effective gain is higher for short pulses if the Kerr lens reduces their beam radius in the gain medium, because then the pulses have a better spatial overlap with the pumped region.

In any case, KLM requires the use of a laser cavity that reacts relatively strongly to changes in the focusing power of the Kerr lens. This is usually achieved only by operating the laser cavity near one of the stability limits, possibly with detrimental effects on the long-term stability.

Detailed modeling of the KLM action requires sophisticated three-dimensional simulation codes, including both the spatial dimensions and the time variable (Cerullo et al., 1996; Christov et al., 1995; Rothenberg, 1992). The basic reason for this is that the strength of the Kerr lens varies within the pulse duration, which leads to complicated spatiotemporal behavior. However, a reasonable understanding can be obtained simply by calculating the transverse cavity modes with a constant Kerr lens, using some averaged intensity value.

Self-starting modelocking with KLM can be achieved with specially optimized laser cavities (Chen et al., 1991; Krausz et al., 1991; Cerullo et al., 1994a, 1994b; Lai, 1994). Unfortunately, this optimization is in conflict with the goal of generating the shortest possible pulses. This is because the laser intensity changes by several orders of magnitude during the transition from cw to mode-locked operation, and the Kerr effect for very short pulses is too strong when the cavity is optimized to react sensitively to long pulses during the start-up phase. Basically one would face a similar problem with any fast saturable absorber, whereas a slow saturable absorber is less critical in this respect because its action depends on pulse energy and not intensity.

Generation of very short pulses—below 6 fs duration—with a self-starting Ti^{3+}:sapphire laser has become possible by combining a SESAM with a cavity set up for KLM (Jung et al., 1997a). The SESAM is then responsible for fast self-starting and the pulse shaping in the femtosecond domain is mainly done by the Kerr effect.

Additive Pulse Modelocking. Before the invention of Kerr lens modelocking, the Kerr effect was used in a different technique called "additive pulse modelocking" (APM) (Kean et al., 1989; Ippen et al., 1989). A cavity containing a single-mode glass fiber is coupled to the main laser cavity. In this cavity, the Kerr effect introduces a larger nonlinear phase shift for the temporal pulse center compared to the wings. When the pulses from both cavities meet again at the coupling mirror, they interfere in such a way that the pulse center is constructively enhanced in the main cavity while its wings are reduced by destructive interference. A prerequisite for this to happen is, of course, that the cavity lengths be equal and stabilized interferometrically. Because other methods (e.g., KLM or the use of saturable absorbers) do not need such stabilization, they are nowadays usually preferred to APM, although APM has been proven to be very effective, particularly in picosecond lasers. For example, the shortest pulses (1.7 ps) from a Nd^{3+}:YAG laser have been achieved with APM (Goodberlet et al., 1990).

A variant of APM that is no longer used is resonant passive modelocking (RPM) (Keller et al., 1990b; 1992b). As with APM, a coupled cavity is used, but this contains a saturable absorber (i.e., an intensity nonlinearity) instead of a Kerr nonlinearity. With this methods, 2 ps pulses were generated with a Ti:sapphire laser (Keller et al., 1990b) and 3.7 ps pulses in a Nd:YLF laser (Keller et al., 1992b).

Nonlinear Mirror Modelocking. Effective saturable absorbers can also be constructed by using $\chi^{(2)}$ nonlinearities (Stankov, 1988). A nonlinear mirror based on this principle consists of a frequency-doubling crystal and a dichroic mirror. For short pulses, part of the incident laser light is converted to the second harmonic, for which the mirror is highly reflective, and converted back to the fundamental wave if an appropriate relative phase shift for fundamental and second harmonic light is applied. On the other hand, unconverted fundamental light experiences a significant loss at the mirror. Thus the device has a higher reflectivity at higher intensities. This has been used for modelocking with, e.g., up to 1.35 W of average output power in 7.9 ps pulses from a $Nd^{3+}:YVO_4$ laser (Agnesi et al., 1997). The achievable pulse duration is often limited by group velocity mismatch between fundamental and second harmonic light.

Q-Switching Instabilities

The usually desired mode of operation is cw modelocking, where a train of pulses with constant parameters (energy, duration, shape) is generated. However, the use of saturable absorbers may also lead to Q-switched modelocking (QML), where the pulse energy oscillates between extreme values (see Fig. 1). The laser then emits bunches of modelocked pulses, which may or may not have a stable Q-switching envelope.

The reason for the QML tendency is the following. Starting from the steady state of cw modelocking, any small increase in pulse energy will lead to stronger saturation of the absorber and thus to a positive net gain. This will lead to exponential growth of the pulse energy until this growth is stopped by gain saturation. In a solid-state laser, which usually exhibits a large gain saturation fluence, this may take many cavity round-tips. The pulse energy will then drop even below the steady-state value. A damped oscillation around the steady state (and finally stable cw modelocking) is obtained only if gain saturation sets in fast enough.

The transition between the regimes of cw modelocking and QML has been investigated in detail (Hönninger et al., 1999; Kärtner et al., 1995b) for slow saturable absorbers. If the absorber is fully saturated, if it always fully recovers between two cavity round-trips, and if soliton shaping effects do not occur, a simple condition for stable cw modelocking can be found (Hönninger et al., 1999a):

$$E_p^2 > E_{L,\mathrm{sat}} E_{A,\mathrm{sat}} \, \Delta R \tag{18}$$

where E_p is the intracavity (not output) pulse energy and $E_{L,\mathrm{sat}}$, $E_{A,\mathrm{sat}}$ are the gain and absorber saturation energies, respectively. Using the saturation parameter $S := E_p / E_{A,\mathrm{sat}}$, we can rewrite this to obtain

$$E_p > E_{L,\mathrm{sat}} \frac{\Delta R}{S} \tag{19}$$

This explains why passively modelocked lasers often exhibit QML when weakly pumped and stable cw modelocking for higher pump powers. Normally, modelocking is fairly stable even for operation only slightly above the QML threshold, so there is no need for operation far above this threshold. The QML threshold is high when $E_{L,\mathrm{sat}}$ is large (laser medium with small laser cross sections and/or large mode area in the gain medium, enforced, e.g., by poor pump beam quality or by crystal fracture), when E_p cannot be made large (limited power of pump source, high repetition rate, or large intracavity losses), or when a high value of ΔR is needed for some reason. We thus find the following prescriptions to avoid QML:

Use a gain medium with small saturation fluence and optimize the pumping arrangement for a small mode area in the gain medium.

Minimize the cavity losses so that a high intracavity pulse energy can be achieved.

Operate the saturable absorber in the regime of strong saturation, although this is limited by the tendency for pulse breakup or by absorber damage.

Do not use a larger modulation depth ΔR than necessary.

Use a cavity with low repetition rate.

Another interesting observation (Hönninger et al., 1999) is that in soliton modelocked lasers the minimum intracavity pulse energy for stable cw modelocking is lower by typically a factor on the order of 4. The reason for this is that a soliton acquires additional bandwidth if its energy increases for some reason. This reduces the effective gain, so that we have a negative feedback mechanism, which tends to stabilize the pulse energy. Thus the use of soliton formation in a laser can help not only to generate shorter pulses but also to avoid QML.

Finally we note that two-photon absorption (which may occur in a SESAM) can modify the saturation behavior in such a way that the QML tendency is reduced (Schibli et al., 2000). In this case, the two-photon absorption acts as an all-optical power limiter (Walker et al., 1986).

Passive Modelocking at High Repetition Rates

The repetition rates of typical modelocked solid-state lasers are on the order of 30–300 MHz. Pulse trains with much higher repetition rates— > 1 GHz or even > 10 GHz—are required for some applications, e.g., in data transmission or for optical clocking of electronic circuits.

It is clear that there are two basic approaches to realizing such high repetition rates: Either one must use a very compact laser cavity, which has a short round-trip time for the circulating pulse, or one must arrange for several pulses to circulate in the cavity with equal temporal spacing. The latter technique, called harmonic modelocking, requires some mechanism to stabilize the pulse spacing. It is widely used in fiber lasers but rarely in solid-state bulk lasers as discussed in this chapter. A Cr^{4+}:YAG laser has been demonstrated with three pulses in the cavity (i.e., harmonic modelocking), resulting in a repetition rate of 2.7 GHz (Collings et al., 1997), which is to our knowledge the highest value achieved with this technique applied to diode-pumped solid-state lasers. A fundamentally modelocked laser with 1.2 GHz repetition rate was also demonstrated (Tomaru et al., 2000).

In the following we concentrate on fundamentally (i.e., not harmonically) modelocked bulk lasers, which have generated repetition rates of up to 77 GHz (Krainer et al., 2000a). It is not difficult to construct a sufficiently compact laser cavity—a cavity length of a few millimeters (or slightly more than 1 mm for 77 GHz) is easily obtained when a compact modelocker such as a SESAM (see earlier) is used. The main challenge is to overcome the tendency for Q-switched modelocking (see previous subsection), which becomes very strong at high repetition rates. Because this issue formerly constituted a challenge even at repetition rates on the order of 1 GHz, specially optimized laser cavities had to be developed for repetition rates > 10 GHz. First it was realized that $Nd^{3+}:YVO_4$ is a laser medium with a particularly high gain cross section of $114 \times 10^{-20}\,\mathrm{cm}^2$ (Peterson et al., 2002). This leads to a small gain saturation energy, which can be further minimized by using a laser cavity with a rather small mode radius of 30 μm or less. Another important factor is to minimize the intracavity losses, so that operation with a small-output coupler transmission and accordingly high intracavity pulse energy is achieved, and to use a SESAM with optimized parameters.

Since the first milestone at 13 GHz (Krainer et al., 1999a), based on a cavity with a Brewster-cut $Nd^{3+}:YVO_4$ crystal, a SESAM, and an air

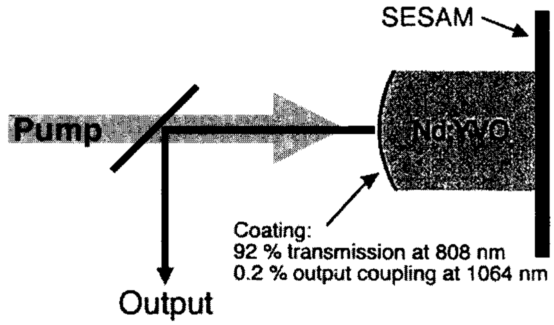

Figure 4 Quasi-monolithic setup as used for Nd^{3+}:YVO_4 lasers with repetition rate above 20 GHz. SESAM: semiconductor saturable absorber mirror.

spacing, quasi-monolithic Nd^{3+}:YVO_4 lasers have been used for higher repetition rates of 29 GHz (Krainer et al., 1999b) and later 59 GHz (Krainer et al., 2000b). Here the laser crystal has a reflective coating on a curved side, and the SESAM is attached to the other end (Fig. 4). In this regime, the repetition rate is limited not only by the Q-switching tendency but also because of the finite pulse duration (typically 5–6 ps), which leads to an increasing overlap of consecutive pulses. However, both limits have been pushed further by employing the effect of soliton modelocking which reduced the pulse duration to 2.7 ps and also has a stabilizing effect, counteracting Q-switching instabilities. The negative dispersion required for soliton modelocking was obtained from a GTI effect (Sec. 1.3.2) generated at a small air gap between the laser crystal and the SESAM. In this way, a repetition rate of 77 GHz was achieved (Krainer et al., 2000a), and further increases even beyond 100 GHz may be possible with this scheme. Note that the average output powers are at least a few tens of milliwatts in all cases, sometimes a few hundred milliwatts. Powers above 1 W at repetition rates of tens of gigahertz appear to be possible with further optimization and are well beyond the foreseeable potential of other approaches, except with external amplification.

Unfortunately, the choice of laser media for high repetition rate at other wavelengths, e.g., 1.5 μm as required for telecom applications, is very limited. Erbium-doped gain media have rather low laser cross sections, which greatly limits their use for passive modelocking at high repetition rates. Cr^{4+}:YAG is more favorable in this respect but suffers from higher crystal losses and a quite variable crystal quality. Repetition rates greater than 10 GHz may still be possible but remain to be demonstrated.

Although we concentrate on lasers based on ion-doped crystals in this chapter, we note that semiconductor gain media are also very interesting for obtaining high pulse repetition rates. The low gain saturation fluence of such a medium basically eliminates the problem of Q-switching instabilities in passively modelocked lasers. The large amplification bandwidth allows for subpicosecond pulse duration, and such devices can be developed for different laser wavelengths. With modelocked edge-emitting semiconductor lasers, repetition rates of up to 1.5 THz (Arahira et al., 1996) have been obtained, but typically at very low power levels and often not with transform-limited pulses. Surface-emitting semiconductor lasers allow for larger mode areas and thus for higher powers, and a good spatial mode quality can be achieved by using an external cavity. Recently, it was recognized that optically pumped surface-emitting semiconductor lasers have a great potential for passive modelocking with multiwatt output power, multigigahertz repetition rates, and possibly subpicosecond pulse durations at the same time. The first passively modelocked lasers of this kind were recently demonstrated (Hoogland et al., 2000), using SESAMs as modelockers. The maximum average output power obtained so far is ≈ 0.2 W, and the pulse durations are typically a few picoseconds, but greatly enhanced performance in terms of output power and pulse duration appears to be feasible in the near future.

Summary: Requirements for Stable Passive Modelocking

Here we briefly summarize a number of conditions that must be met to obtain stable passive modelocking:

- The laser must have a good spatial beam quality, i.e., it must operate in the fundamental transverse mode (see Sec. 1.4.1).
- The saturable absorber must be strong and fast enough that the loss difference between the pulses and a cw background is sufficient to compensate for the smaller effective gain of the short pulses.
- The saturable absorber must be strong enough to guarantee stable self-starting. (A longer absorber recovery times helps in this respect, see earlier in this section.)
- The absorber should not be too strongly saturated, because this would introduce a tendency for double pulses, particularly in the soliton regime. The effective gain is larger for double pulses (with decreased energy and bandwidth), and a strongly saturated absorber cannot sufficiently favor the more energetic single pulses.
- Nonlinear phase shifts from self-phase modulation must not be too strong, particularly in cases with zero or positive dispersion. In the soliton mode-locked regime, significantly stronger self-phase modulation can be tolerated and is even desirable.

To avoid Q-switching instabilities, the condition discussed earlier in this section must be fulfilled.

In some cases where inhomogeneous gain saturation occurs [e.g., induced by spatial hole burning (Braun et al., 1995, Kärtner et al., 1995c, Paschotta et al., 2001)], spectral stability may not be achievable. A spectral hole in the gain, generated by the current lasing spectrum, can lead to a situation where a shift of the gain spectrum to longer or shorter wavelengths increases the gain. Such a situation is unstable and must be avoided, possibly by the use of a suitable intracavity filter.

1.5 DESIGNS OF MODELOCKED LASERS

In the preceding sections we discussed the most important physical effects that are relevant for the operation of modelocked lasers. Here we give an overview on laser designs, with emphasis on those designs that are currently used and/or promise to find widespread application in the foreseeable future. We discuss a number of practical aspects for the design and operation of such lasers.

1.5.1 Picosecond Lasers

The setups of picosecond lasers typically do not differ very much from those of lasers for continuous-wave operation. Some modelocker is installed, which might be either an acousto-optic modulator (AOM) for active modelocking (Sec. 1.4.2) or, e.g., a SESAM (Sec. 1.4.3) for passive modelocking. Also, the cavity design needs to fulfill a few additional demands. As an example, we refer to Figure 5, which shows the setup of a high-power Nd^{3+}:YAG laser (Spühler et al., 1999b), passively modelocked with a SESAM. The cavity design must provide appropriate beam radii both in the laser head (where the fundamental Gaussian mode should just fill the

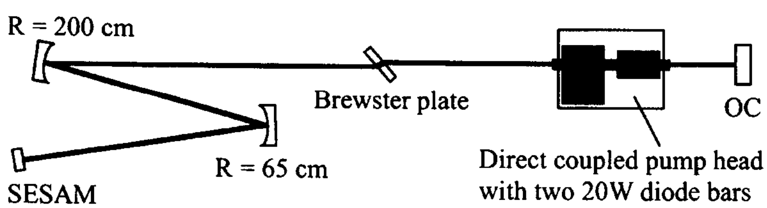

Figure 5 Setup of passively modelocked high-power Nd^{3+}: YAG laser, containing a DCP laser head, two curved mirrors, a SESAM, and an output coupler mirror (OC) with 7% transmission.

usable area) and on the SESAM, so as to use an appropriate degree of saturation. The latter depends on a number of factors: the output power, the output coupler transmission, the cavity length, and the saturation fluence of the SESAM. Obviously the cavity length must be chosen to obtain the desired repetition rate. The equations given in Section 1.4.3 can be used to ensure that the chosen design will not suffer from Q-switching instabilities. The laser head is side-pumped in the mentioned example, but end-pumped laser heads can also be used, where the pump light is typically injected through a folding mirror that is highly reflective for the laser light.

The SESAM should typically be used as an end mirror, not as a folding mirror. Otherwise a tendency for the generation of multiple pulses, which would meet on the SESAM, might be induced.

Similar setups can be used for actively modelocked lasers, where the SESAM is replaced by an AOM. The AOM should be placed close to an end mirror, for reasons similar to those discussed above for the SESAM.

1.5.2 High-Power Thin-Disk Laser

By far the highest average powers in the subpicosecond domain can be obtained from thin-disk Yb^{3+}:YAG lasers, passively modelocked with a SESAM: 16.2 W in 700 fs pulses has been demonstrated (Aus der Au et al., 2000). The thin-disk laser head (Giesen et al., 1994) is power-scalable because of the nearly one-dimensional heat flow in the beam direction: Thermal effects (such as thermal lensing) do not become more severe if the mode area is scaled up in proportion to the power level. The same is true for the SESAM (Sec. 1.4.3), which also has the geometry of a thin disk. Thus the whole concept of the passively modelocked thin-disk laser is power-scalable, and average power levels above 50 W are expected for the near future.

Because the thin disk must be cooled from one side, a reflecting coating on this side is used, and the laser beam is always reflected at the disk. For modelocked operation, the disk is preferably used as a folding mirror rather than as an end mirror, because the two ends of the standing-wave cavity are then available for the output coupler mirror and the SESAM. An appropriate amount of negative dispersion for soliton modelocking (Sec. 1.4.3) is generated with a GTI (Sec. 1.3.2) or with a dispersive mirror. Prism pairs (Sec. 1.3.2) appear to be unsuitable because either they absorb too highly (and thus exhibit thermal lensing), as, e.g., for SF10 glass, or they do not provide sufficient dispersion (as for silica). Soliton modelocked operation is essential because otherwise the pulse duration would be longer and the modelocking operation would be destabilized by the action by spatial hole burning (Paschotta et al., 2001). Also, it helps to suppress Q-switching instabilities (Sec. 1.4.3) (see also Hönninger et al., 1999).

1.5.3 Typical Femtosecond Lasers

Most femtosecond lasers are based on an end-pumped laser setup, with a broadband laser medium such as Ti^{3+}:sapphire, Cr^{3+}:LiSAF, or Yb^{3+}:glass (see Sec. 1.2 for an overview). In the case of Ti^{3+}:sapphire, the pump source can be either an argon ion laser or a frequency-doubled solid-state laser. In any case, one typically uses a few watts of pump power in a beam with good transverse beam quality, because the mode radius in the Ti^{3+}:sapphire rod is usually rather small. Other gain media such as Cr^{3+}:LiSAF or Yb^{3+}:glass are typically pumped with high-brightness diode lasers, delivering a few watts with beam quality M^2 factor on the order of 10 in one direction and <5 in the other direction.

Typically laser cavities (see Fig. 6 as an example) contain two curved mirrors within a distance of a few centimeters on opposite sides of the gain medium. The pump power is usually injected through one or both of these mirrors, which also focus the intracavity laser beam to an appropriate beam waist. One of the two "arms" of the cavity ends with the output coupler mirror, and the other one may be used for a SESAM as a passive mode-locker. One arm typically contains a prism pair (Sec. 1.3.2) for dispersion compensation, which is necessary for femtosecond pulse generation. In practically all cases, femtosecond lasers operate in the regime of negative overall intracavity dispersion so that soliton-like pulses are formed.

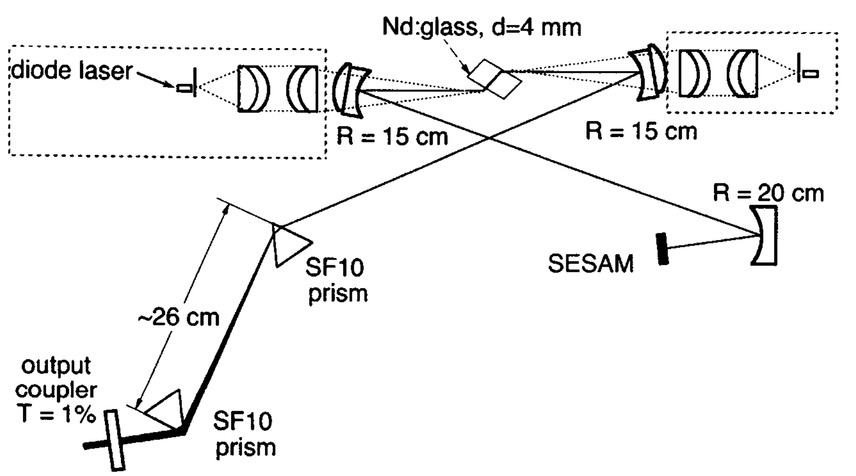

Figure 6 Setup of a femtosecond Nd:glass laser (Aus der Au et al., 1997). The gain medium is pumped with two laser diodes. A prism pair is used for dispersion compensation, and a SESAM as modelocker. This laser generated 60 fs pulses with 84 mW average power.

Instead of a SESAM, or in addition to it, the Kerr lens in the gain medium can be used for modelocking (Sec. 1.4.3). In most cases, soft-aperture KLM is used. Here, the cavity design is made such that the Kerr lens reduces the mode area for high intensities and thus improves the overlap with the (strongly focused) pump beam. This is achieved by operating the laser cavity near one of the stability limits of the cavity, which are found by varying the distance between the above-mentioned curved folding mirrors or some other distance in the cavity.

For the shortest pulse durations around 5–6 fs (Morgner et al., 1999b; Sutter et al., 2000), the strong action of KLM as an effective fast saturable absorber is definitely required. Also double-chirped mirrors (Sec. 1.3.2) are required for precise dispersion compensation over a very broad bandwidth. Typically, several dispersive mirrors are used in the laser cavity, and additional mirrors are used for further external compression. A SESAM allows for self-starting modelocking (Jung et al., 1997a).

Higher pulse energies and peak powers have been generated by using laser setups with reduced repetition rates of, e.g., 15 MHz (Cho et al., 1999). The long cavity length required for such repetition rates is achieved by inserting a multipass cell. However, the limiting factor to the pulse energy is ultimately not the practically achievable cavity length but rather the nonlinearity of the gain crystal—at least in the sub-30 fs domain: If self-phase modulation becomes too strong, this destabilizes the modelocking process.

1.5.4 Lasers with High Repetition Rates

For ultrashort pulses with multigigahertz repetition rate, laser designs are required that are very different from those described in the previous sections. We discussed such designs with up to 77 GHz repetition rate in Section 1.4.3. Another type of laser in this domain is described in the next section.

1.5.5 Passively Modelocked Optically Pumped Semiconductor Lasers

Here we discuss a novel type of modelocked laser that is based not on an ion-doped crystal or glass as gain medium, but on a semiconductor medium. This special case of a modelocked semiconductor laser is described here because it allows for much higher output powers than other modelocked semiconductor lasers and can thus be compared directly with ion-doped lasers. The gain medium is a surface-emitting semiconductor chip, with a Bragg mirror and one or several amplifying quantum wells grown on a wafer (made, e.g., of GaAs). The diffraction-limited laser mode is formed in an external cavity that also contains a SESAM (Sec. 1.4.3) for passive modelocking. Optical pumping of the gain medium allows the use of a rather large mode with correspondingly high output power. If the cooling (e.g., through the GaAs substrate, which may be thinned down) is sufficient, the output power can be scaled by increasing the mode area so that the temperature is not increased. Thus we have a power-scalable concept that should allow for multiwatt average output powers. Q-switching instabilities (Sec. 1.4.3) do not occur because of the small saturation fluence of the semiconductor gain medium, so very high repetition rates can be achieved. The gain bandwidth is sufficient for the generation of subpicosecond pulses.

Since the first demonstration of this concept (Hoogland et al., 2000), the average output power has been increased to >200 mW (Häring et al., 2001), and further increases should be possible soon. The pulse durations have so far been at least a few picoseconds, but shorter pulses should also become possible. We envisage that this concept will lead to lasers with multigigahertz repetition rates, multiwatt output powers, and subpicosecond pulse durations. This combination of properties would be very difficult to achieve with ion-doped gain media.

1.6 PASSIVELY Q-SWITCHED MICROCHIP LASERS

Ultrashort pulses are in most cases generated with modelocked lasers of some kind. Q-switching is a method that is typically used to generate much longer pulses (>1 ns pulse duration). This is because the pulse duration achievable with Q-switching is longer than the cavity round-trip time, which is typically a few nanoseconds. The achievable pulse energy is significantly higher than with modelocking, because the repetition rate is relatively low. Another feature is that the output linewidth can be rather small; in some cases the emission is limited to a single cavity mode.

A very compact laser setup can be obtained using the principle of a microchip laser (Zayhowski et al., 1989). In such a setup (Fig. 7), a thin disk of a gain medium (and optionally a modulator) is sandwiched between two mirrors. Because the round-trip time can be far lower than 1 ns, Q-switched pulses from such a laser can be much shorter than pulses from conventional Q-switched lasers.

The first Q-switching result for a microchip laser was obtained in 1992 with an electro-optic modulator in the cavity. In this way, 115 ps pulses were generated (Zayhowski et al., 1992). With a Cr^{4+}:YAG absorber for passive Q-switching, the shortest pulse duration was 218 ps (Zayhowski, 1996). Further shortening of the cavity, and consequently a pulse duration to 56 ps, were achieved in 1997 by passive Q-switching with a SESAM (Sec. 1.4.3) (Braun et al., 1997). The cavity length is then basically determined by the thickness of the laser crystal, because the penetration depth in the

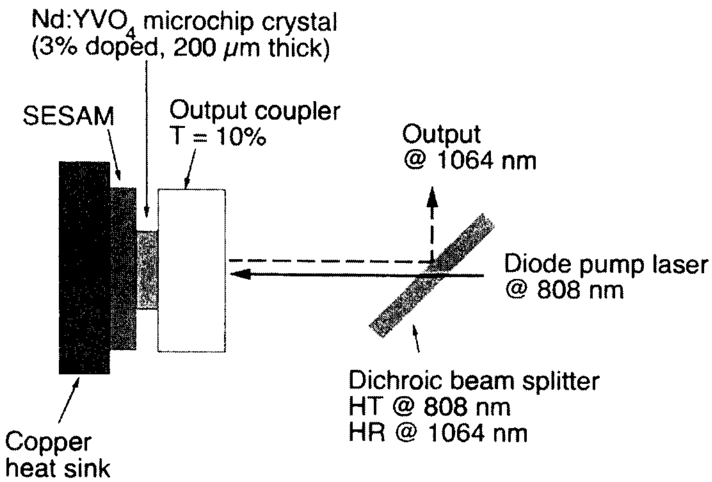

Figure 7 Setup of a Nd :YVO_4 microchip laser that is passively Q-switched with a SESAM. The Nd:YVO_4 crystal is sandwiched between the SESAM and the output coupler mirror. A dichroic mirror is used to separate the output beam from the pump beam.

SESAM is only a few micrometers. Optimization of various parameters of a Nd^{3+}:YVO_4 laser led to the shortest pulses of 37 ps duration (Spühler et al., 1999c). Although such pulse durations are comparable to those of many modelocked lasers, other parameters are quite different. In particular, the repetition rate of Q-switched microchip lasers is much lower; it can be varied in a wide range from a few hundred hertz to a few megahertz and depends on the pumping conditions (pump power and spot size). The pulse energy can well exceed a microjoule in some cases. Such pulses are very suitable for range finding, for example, where subnanosecond pulse durations at a low repetition rate are desired and some fluctuations of the repetition rate can be tolerated. If operation on a single transverse cavity mode can be achieved (as is the case for a thin enough gain medium), these fluctuations can be fairly small (a few percent or less).

For calculation of the main operation parameters, a simple set of equation has been derived (Spühler et al., 1999c). These equations are based on a number of approximations, which are typically well fulfilled in real lasers and have been tested experimentally. Here we briefly summarize the results. According to

$$\tau_p \approx 3.5 \frac{T_r}{\Delta R} \tag{20}$$

the pulse duration τ_p depends only on the cavity round-trip time T_r and the modulation depth ΔR of the SESAM. The output pulse energy E_p depends on the modulation depth and the saturation energy $E_{L,\mathrm{sat}} = h\nu_L A_L/\sigma_{\mathrm{em}}$ (with the emission cross section σ_{em}, assuming a four-level system) of the laser medium:

$$E_p \approx E_{L,\mathrm{sat}}\,\Delta R \tag{21}$$

The laser mode area A_L is defined by the pumping conditions, which determine the strength of the thermal lens in the gain medium. A_L can be varied in a certain range by adjusting the spot size of the pump beam. For Eqs. (20) and (21) to be valid, it is assumed that ΔR is not larger than the sum of the liner cavity losses, which leads to a nearly symmetrical temporal shape of the pulses.

The pulse repetition rate is simply obtained by dividing the average output power by the pulse energy. This shows that the repetition rate is a linear function of the pump power, provided that the laser mode area stays approximately constant.

To generate rather short pulses, a thin gain crystal has to be combined with a SESAM with high modulation depth. It is thus important to choose a highly doped crystal with a high gain per unit length and short pump absorption length. Nd^{3+}:YVO_4 has proven to be very suitable for this purpose.

For high pulse energies, gain media with large saturation fluence are ideal. An Yb^{3+}:YAG microchip laser generated 1.1 μJ pulses of 0.53 ns duration at 1030 nm (Spühler et al., 2001), and up to 4 μJ in subnanosecond pulses in the eye-safe wavelength regime around $\approx 1.5\,\mu\mathrm{m}$ have been obtained with Er^{3+}:Yb^{3+}:glass (Fluck et al., 1998). In this case, the limits are set by SESAM damage, because the obtained intracavity pulse fluence is much higher than the SESAM saturation fluence, even with optimized high-finesse SESAM designs. On the other hand, the laser mode area cannot be easily scaled up because of the requirement that the thermal lens form a stable cavity mode.

An interesting feature of the passively Q-switched microchip laser is that the pulse parameters (energy, duration, shape) are very stable, because they are determined only by fixed properties of the cavity, the gain medium, and the saturable absorber. The pump power basically influences only the pulse repetition rate, because the formation of a pulse is always triggered when a certain fixed level of stored energy (and thus gain) is reached. Apart from this, only weak fluctuations of the pulse energy may be expected if fluctuations of the pump power translate into slight changes of the laser mode area. The situation is different for actively Q-switched microchip lasers; here the repetition rate is electronically determined, whereas the pulse parameters (energy, duration, shape) depend on the energy stored in the gain medium at the moment the pulse is triggered. Therefore, the pulse parameters are affected by low-frequency pump power fluctuations.

1.7 SUMMARY AND OUTLOOK

We have shown that the technology of ultrafast lasers has become very refined and is now suitable for application in many areas. Points of particular importance in this respect are:

- The transition from dye lasers to solid-state lasers, which can be compact, powerful, efficient, and long-lived. It has been shown that solid-state lasers can generate pulses that are even shorter than those generated in dye lasers.
- The development of diode lasers for direct pumping of solid-state lasers. This has led not only to very efficient and compact lasers, but also to modelocked lasers with tens of watts of output power.
- The development of semiconductor saturable absorbers that can be optimized for operation in very different parameter regimes concerning laser wavelength, pulse duration, and power levels.

Within the next few years we expect the following developments in the filed:

- New solid-state gain media will be used. In particular, Cr^{2+}:ZnSe (see Sec. 1.2) appears to be suitable for the generation of pulses of 20 fs duration or less in a new spectral region around 2.7 μm.
- Very high power levels (tens of watts or even >100 W of average power) should become possible with passively modelocked thin-disk lasers. Pulse durations just below 1 ps are already feasible in this power regime, but with new materials the regime of 200 fs or even below should become accessible with similarly high powers. Amplifier devices for lower repetition rates will become important for material processing.
- Nonlinear frequency conversion stages (based on second harmonic generation, sum frequency mixing, or parametric oscillation) will be pumped with high-power modelocked lasers to generate short, powerful pulses at other wavelengths. This will be of interest, e.g., for application in large-screen RGB display systems.
- As an alternative to ion-doped gain media, optically pumped semiconductor lasers with an external cavity and a SESAM for passive modelocking (Sec. 1.5.5) will generate higher output powers and shorter pulses in the regime of multigigahertz pulse repetition rates.

We thus believe that the development of ultrafast laser sources has not come to its end but will continue to deliver new devices with superior properties for many applications.

ACKNOWLEDGMENTS

We thank T. Südmeyer for help with the preparation of the manuscript.

REFERENCES

Agnesi A, Pennacchio C, Reali GC, Kubecek V. (1997). High-power diode-pumped picosecond Nd:YVO_4 laser. Opt Lett 22:1645–1647.

Aus der Au J, Kopf D, Morier-Genoud F, Moser M, Keller U. (1997). 60-fs pulses from a diode-pumped Nd:glass laser. Opt Lett 22:307–309.

Aus der Au J, Loesel FH, Morier-Genoud F, Moser M, Keller U. (1998). Femtosecond diode-pumped Nd:glass laser with more than 1-W average output power. Opt Lett 23:271–273.

Aus der Au J, Schaer SF, Paschotta R, Hönninger C, Keller U, Moser M. (1999). High-power diode-pumped passively modelocked Yb:YAG lasers. Opt Lett 24:1281–1283.

Aus der Au J, Spühler GJ, Südmeyer T, Paschotta R, Hövel R, Moser M, Erhard S, Karszewski M, Giesen A, Keller U. (2000). 16.2 W average power from a diode-pumped femtosecond Yb:YAG thin disk laser. Opt Lett 25:859.

Bado P, Bouvier M, Coe JS. (1987). Nd:YLF mode-locked oscillator and regenerative amplifier. Opt Lett 12:319–321.

Baltuska A, Wei Z, Pshenichnikov MS, Wiersma DA, Szipöcs R. (1997). All-solid-state cavity dumped sub-5-fs laser. Appl Phys B 65:175–188.

Bartels A, Dekorsky T, Kurz H. (1999). Femtosecond Ti:sapphire ring laser with 2-GHz repetition rate and its application in time-resolved spectroscopy. Opt Lett 24:996–998.

Basu S, Byer RL. (1988). Continuous-wave mode-locked Nd:glass laser pumped by a laser diode. Opt Lett 13:458–460.

Becker MF, Kuizenga KJ, Siegman AE. (1972). Harmonic mode locking of the Nd:YAG laser. IEEE J Quantum Electron QE-8:687–693.

Beddard T, Sibbett W, Reid DT, Garduno-Mejia J, Jamasbi N, Mohebi M. (1999). High-average-power, 1-MW peak-power self-mode-locked Ti:sapphire oscillator. Opt Lett 24:163–165.

Blow KJ, Nelson BP. (1988). Improved modelocking of an F-center laser with a nonlinear nonsoliton external cavity. Opt Lett 13:1026–1028.

Braun B, Hönninger C, Zhang G, Keller U, Heine F, Kellner T, Huber G. (1996). Efficient intracavity frequency doubling of a passively modelocked diode-pumped Nd:LSB laser. Opt Lett 21:1567–1569.

Brovelli LR, Jung ID, Kopf D, Kamp M, Moser M, Kärtner FX, Keller U. (1995). Self-starting soliton modelocked Ti:sapphire laser using a thin semiconductor saturable absorber. Electron Lett 31:287–289.

Brunner F, Spühler GJ, Aus der Au J, Krainer L, Morier-Genoud F, Paschotta R, Lichtenstein N, Weiss S, Harder C, Lagatsky AA, Abdolvand A, Kuleshov NV, Keller U. (2000). Diode-pumped femtosecond Yb:KGd$(WO_4)_2$ laser with 1.1-W average power. Opt Lett 25:1119–1121.

Burns D, Hetterich M, Ferguson AI, Bente E, Dawson MD, Davies JI, Bland SW. (2000). High-average-power (> 20 W) Nd:YVO_4 lasers mode locked by strain-compensated saturable Bragg reflectors. J Opt Soc Am B 17:919–926.

Carrig TJ, Wagner GJ, Sennaroglu A, Jeong JY, Pollock CR. (2000). Mode-locked Cr^{2+}:ZnSe laser. Opt Lett 25:168–170.

Cerullo G, Dienes A, Magni V. (1996). Space-time coupling and collapse threshold for femtosecond pulses in dispersive nonlinear media. Opt Lett 21:65–67.

Cho SH, Bouma BE, Ippen EP, Fujimoto JG. (1999). Low-repetition-rate high-peak-power Kerr-lens mode-locked Ti:Al_2O_3 laser with a multiple-pass cell. Opt Lett 24:417–419.

Christov IP, Stoev VD, Murnane MM, Kapteyn HC. (1995). Mode locking with a compensated space-time astigmatism. Opt Lett 20:2111–2113.

Chudoba C, Fujimoto JG, Ippen EP, Haus HA, Morgner U, Kärtner FX, Scheuer V, Angelow G, Tschudi T. (2000). All-solid-state Cr:forsterite laser generating 14-fs pulses at 1.3 μm. Conf. on Lasers and Electro-Optics, 2000, Postdeadline paper CPD4.

Collings BC, Stark JB, Tsuda S, Knox WH, Cunningham JE, Jan WY, Pathak R, Bergman K. (1996). Saturable Bragg reflector self-starting passive modelocking of a Cr^{4+}:YAG laser pumped with a diode-pumped Nd:YVO_4 laser. Opt Lett 21:1171–1173.

Couderc V, Louradour F, Barthelemy A. (1999). 2.8 ps pulses from a modelocked diode pumped Nd:YVO_4 laser using quadratic polarization switching. Opt Commun 166:103–111.

Curley PF, Ferguson AI. (1991). Actively modelocked Ti:sapphire laser producing transform-limited pulses of 150 fs duration. Opt Lett 16:1016–1018.

De Maria AJ, Stetser DA, Heynau H. (1966). Self mode-locking of lasers with saturable absorbers. Appl phys Lett 8:174–176.

Diels JC, Stryland EWV, Benedict G. (1978). Generation and measurement of pulses of 0.2 ps duration. Opt Commun 25:93.

Druon F, Balembois F, Georges P, Brun A, Courjaud A, Hönninger C, Salin F, Aron A, Mougel F, Aka G, Vivien D. (2000). Generation of 90-fs pulses from a modelocked diode-pumped Yb:$Ca_4GdO(Bo_3)_3$ laser. Opt Lett 25:423–425.

Fluck R, Zhang G, Keller U, Weingarten KJ, Moser M. (1996). Diode-pumped passively mode-locked 1.3 μm Nd:YVO_4 and Nd:YLF lasers by use of semiconductor saturable absorbers. Opt Lett 21:1378–1380.

Fork RL, Cruz CHB, Becker PC, Shank CV. (1987). Compression of optical pulses to six femtoseconds by using cubic phase compensation. Opt Lett 12:483–485.

Fork RL, Greene BI, Shank CV. (1981). Generation of optical pulses shorter than 0.1 ps by colliding pulse modelocking. Appl Phys Lett 38:617–619.

Fork RL, Martinez OE, Gordon JP. (1984). Negative dispersion using pairs of prisms. Opt Lett 9:150–152.

French PMW, Mellish R, Taylor JR, Delfyett PJ, Florez LT. (1993). Modelocked all-solid-state diode-pumped Cr:LiSAF laser. Opt Lett 18:1934–1936.

Gabel KM, Russbuldt P, Lebert R, Valster A. (1998). Diode-pumped Cr^{3+}:LiCAF fs-laser. Opt Commun 157:327–334.

Giesen A, Hügel H, Voss A, Wittig K, Brauch U, Opower H. (1994). Scalable concept for diode-pumped high-power solid-state lasers. Appl Phys B 58:363–372.

Gires F, Tournois P. (1964). Interferometre utilisable pour la compression d'impulsions lumineuses modulees en frequence. CR Acad Sci Paris 258:6112–6115.

Gloster LAW, Cormont P, Cox AM, King TA, Chain BHT. (1997). Diode-pumped Q-switched Yb:S-FAP laser. Opt Commun. 146:177–180.

Godil AA, Hou A, Auld BA, Bloom DM. (1991). Harmonic mode locking of a Nd: BEL laser using a 20-GHZ dielectric resonator/optical modulator. Opt Lett 16:1765–1767.

Goodberlet J, Jacobson J, Fujimoto JG, Schulz PA, Fan TY. (1990). Self-starting additive pulse modelocked diode-pumped Nd:YAG laser. Opt Lett 15:504–506.

Goodberlet J, Wang J, Fujimoto JG, Schulz PA. (1989). Femtosecond passively mode-locked Ti:sapphire laser with a nonlinear external cavity. Opt Lett 14:1125–1127.

Haiml M, Siegner U, Morier-Genoud F, Keller U, Luysberg M, Lutz RC, Specht P, Weber ER. (1999b). Optical nonlinearity in low-temperature grown GaAs: microscopic limitations and optimization strategies. Appl Phys Lett 74:3134–3136.

Haiml M, Siegner U, Morier-Genoud F, Keller U, Luysberg M, Specht P, Weber ER. (1999a). Femtosecond response times and high optical nonlinearity in beryllium doped low-temperature grown GaAs. Appl Phys Lett 74:1269–1271.

Hargrove LE, Fork RL, Pollack MA. (1964). Locking of HeNe laser modes induced by synchronous intracavity modulation. Appl Phys Lett 5:4.

Haus HA, Keller U, Knox WH. (1991). A theory of coupled cavity modelocking with resonant nonlinearity. J Opt Soc Am B 8:1252–1258.

Henrich B, Beigang R. (1997). Self-starting Kerr-lens mode locking of a Nd:YAG-laser. Opt Commun 135:300–304.

Hönninger C, Morier-Genoud F, Moser M, Keller U, Brovelli LR, Harder C. (1998). Efficient and tunable diode-pumped femtosecond Yb:glass lasers. Opt Lett 23:126–128.

Hönninger C, Paschotta R, Graf M, Morier-Genoud F, Zhang G, Moser M, Biswal S, Nees J, Braun A, Mourou GA, Johannsen I, Giesen A, Seeber W, Keller U. (1999b). Ultrafast ytterbium-doped bulk lasers and laser amplifiers. Appl Phys B 69:3–17.

Hönninger C, Zhang G, Keller U, Giesen A. (1995). Femtosecond Yb:YAG laser using semiconductor saturable absorbers. Opt Lett 20:2402–2404.

Hönninger C, Paschotta R, Morier-Genoud F, Moser M, Keller U. (1999a). Q-switching stability limits of continuous-wave passive mode locking. J Opt Soc Am B 16:46–56.

Hughes DW, Barr JRM, Hanna DC. (1991). Mode locking of a diode-laser-pumped Nd:glass laser by frequency modulation. Opt Lett 16:147–149.

Hughes DW, Phillips MW, Barr JRM, Hanna DC. (1992). A laser-diode-pumped Nd:glass laser: mode-locked, high-power, and single frequency performance. IEEE J Quantum Electron 28:1010–1017.

Ippen EP, Haus HA, Liu LY. (1989). Additive pulse modelocking. J Opt Soc Am B 6:1736–1745.

Islam MN, Sunderman ER, Soccolich CE, Bar-Joseph I, Sauer N, Chang TY, Miller BL. (1989). Color center lasers passively mode locked by quantum wells. IEEE J Quantum Electron 25:2454–2463.

Jeong TM, Kang EC, Nam CH. (1999). Temporal and spectral characteristics of an additive-pulse mode-locked Nd:YLF laser with Michelson-type configuration. Opt Commun 166:95–102.

Juhasz T, Lai ST, Pessot MA. (1990). Efficient short-pulse generation from a diode-pumped Nd: YLF laser with a piezoelectrically induced diffraction modulator. Opt Lett 15:1458–1460.

Jung ID, Brovelli LR, Kamp M, Keller U, Moser M. (1995a). Scaling of the antiresonant Fabry-Perot saturable absorber design toward a thin saturable absorber. Opt Lett 20:1559–1561.

Jung ID, Kärtner FX, Brovelli LR, Kamp M, Keller U. (1995b). Experimental verification of soliton modelocking using only a slow saturable absorber. Opt Lett 20:1892–1894.

Jung ID, Kärtner FX, Matuschek N, Sutter DH, Morier-Genoud F, Zhang G, Keller U, Scheuer V, Tilsch M, Tschudi T. (1997). Self-starting 6.5 fs pulses from a Ti:sapphire laser. Opt Lett 22:1009–1011.

Kärtner FX, Aus der Au J, Keller U. (1998). Modelocking with slow and fast saturable absorbers: what's the difference? IEEE J Selected Topics Quantum Electron 4:159–168.

Kärtner FX, Jung ID, Keller U. (1996). Soliton modelocking with saturable absorbers. Special Issue on Ultrafast Electronics, Photonics and Optoelectronics, IEEE J Selected Topics Quantum Electron (JSTQE) 2:540–556.

Kärtner FX, Keller U. (1995). Stabilization of soliton-like pulses with a slow saturable absorber. Opt Lett 20:16–18.

Kärtner FX, Matuschek N, Schibli T, Keller U, Haus HA, Heine C, Morf R, Scheuer V, Tilsch M, Tschudi T. (1997). Design and fabrication of double-chirped mirrors. Opt Lett 22:831–833.

Kean PN, Zhu X, Crust DW, Grant RS, Landford N, Sibbett W. (1989). Enhanced modelocking of color center lasers. Opt Lett 14:39–41.

Keller U. (1994). Ultrafast all-solid-state laser technology. Appl Phys B 58:347–363.

Keller U. (1999). Semiconductor nonlinearities for solid-state laser modelocking and Q-switching, in Nonlinear Optics in Semiconductors, A. Kost and E. Garmire (eds.), Boston: Academic Press, pp. 211–286.

Keller U. (2001). Short and Ultra short Pulse Generation, in Laser Physics and Application, G. Herzinfer, R. Poprawe, H. Weber (eds.), Springer, 2002.

Keller U, Chiu TH. (1992b). Resonant passive modelocked Nd: YLF laser. IEEE J Quantum Electron 28:1710–1721.

Keller U, Knox WH, Roskos H. (1990b). Coupled-cavity resonant passive mode-locked (RPM) Ti:sapphire laser. Opt Lett 15:1377–1379.

Keller U, Li KD, Khuri-Yakub BT, Bloom DM, Weingarten KJ, Gerstenberger DC. (1990a). High-frequency acousto-optic modelocker for picosecond pulse generation. Opt Lett 15:45–47.

Keller U, Miller DAB, Boyd GD, Chiu TH, Ferguson JF, Asom MT. (1992a). Solid-state low-loss intracavity saturable absorber for Nd:YLF lasers: an antiresonant semiconductor Fabry-Perot saturable absorber. Opt Lett 17:505–507.

Keller U, Valdmanis JA, Nuss MC, Johnson AM. (1988). 53 ps pulses at 1.32 μm from a harmonic mode-locked Nd:YAG laser. IEEE J Quantum Electron 24:427–430.

Keller U, Weingarten KJ, Kärtner FX, Kopf D, Braun B, Jung ID, Fluck R, Hönninger C, Matuschek N, Aus der Au J. (1996). Semiconductor saturable absorber mirrors (SESAMs) for femtosecond to nanosecond pulse generation in solid-state lasers. IEEE J Selected Topics Quantum Electron 2:435–453.

Kopf D, Kärtner FX, Weingarten KJ, Keller U. (1995b). Diode-pumped mode-locked Nd:glass lasers using an A-FPSA. Opt Lett 20:1169–1171.

Kopf D, Kärtner F, Weingarten KJ, Keller U. (1994b). Pulse shortening in a Nd:glass laser by gain reshaping and soliton formation. Opt Lett 19:2146–2148.

Kopf D, Spühler GJ, Weingarten KJ, Keller U. (1996b). Mode-locked laser cavities with a single prism for dispersion compensation. Appl Opt 35:912–915.

Kopf D, Weingarten KJ, Brovelli LR, Kamp M, Keller U. (1994a). Diode-pumped 100-fs passively mode-locked Cr:LiSAF laser with an antiresonant Fabry-Perot saturable absorber. Opt Lett 19:2143–2145.

Kopf D, Weingarten KJ, Brovelli LR, Kamp M, Keller U. (1995a). Sub-50-fs diode-pumped mode-locked Cr:LiSAF with an A-FPSA. Conference on Lasers and Electro-Optics.

Kopf D, Weingarten KJ, Zhang G, Moser M, Emanuel MA, Beach RJ, Skidmore JA, Keller U. (1997). High-average-power diode-pumped femtosecond Cr:LiSAF lasers. Appl Phys B 65:235–243.

Kopf D, Zhang G, Fluck R, Moser M, Keller U. (1996a). All-in-one dispersion-compensating saturable absorber mirror for compact femtosecond laser sources. Opt Lett 21:486–488.

Krainer L, Paschotta R, Moser M, Keller U. (2000). 77 GHz soliton modelocked $Nd:YVO_4$ laser. Electron Lett 36:1846–1848.

Kubecek V, Couderc V, Bourliaguet B, Louradour F, Barthelemy A. (1999). 4-W and 23-ps pulses from a lamp-pumped Nd:YAG laser passively mode-locked by polarization switching in a KTP crystal. Appl Phys B 69:99–102.

Larionov M, Gao J, Erhard S, Giesen A, Contag K, Peters V, Mix E, Fornasiero L, Petermann K, Huber G, Aus der Au J, Spühler GJ, Paschotta R, Keller U, Lagatsky AA, Abdolvand A, Kuleshov NV. (2001). Thin disk laser operation and spectroscopic characterization of Yb-doped sesquioxides and potassium tungstates. Advanced Solid State Lasers. Vol. 50, P. 625.

Li KD, Sheridan JA, Bloom DM. (1991). Picosecond pulse generation in Nd:BEL with a high-frequency acousto-optic mode locker. Opt Lett 16:1505–1507.

LiKamWa P, Chai BHT, Miller A. (1992). Self-mode-locked Cr^{3+}:$LiCaAlF_6$ laser. Opt Lett 17:1438–1440.

Lincoln JR, Ferguson AI. (1994). All-solid-state self-mode locking of a Nd:YLF laser. Opt Lett 19:2119–2121.

Liu JM, Chee JK. (1990b). Passive modelocking of a cw Nd:YLF laser with a non-linear external coupled cavity. Opt Lett 15:685–689.

Liu KX, Flood CJ, Walker DR, Driel HMv. (1992). Kerr lens mode locking of a diode-pumped Nd:YAG laser. Opt Lett 17:1361–1363.

Liu LY, Huxley JM, Ippen EP, Haus HA. (1990a). Self-starting additive pulse mode-locking of a Nd:YAG laser. Opt Lett 15:553–555.

Loesel FH, Horvath C, Grasbon F, Jost M, Niemz MH. (1997). Selfstarting femtosecond operation and transient dynamics of a diode-pumped Cr:LiSGaF laser with a semiconductor saturable absorber mirror. Appl Phys B 65:783–787.

Maker GT, Ferguson AI. (1989a). Frequency-modulation mode locking of diode-pumped Nd:YAG laser. Opt Lett 4:788–790.

Maker GT, Ferguson AI. (1989b). Electron Lett 25:1025.

Maker GT, Ferguson AI. (1989c). Modelocking and Q-switching of a diode laser pumped neodymium-doped yttrium lithium fluoride laser. Appl Phys Lett 54:403–405.

Malcolm GPA, Curley PF, Ferguson AI. (1990). Additive pulse modelocking of a diode pumped Nd:YLF laser. Opt Lett 15:1303–1305.

Mellish PM, French PMW, Taylor JR, Delfyett PJ, Florez LT. (1994). All-solid-state femtosecond diode-pumped Cr:LiSAF laser. Electron Lett 30:223–224.

Miller A, LiKamWa P, Chai BHT, Stryland EWV. (1992). Generation of 150-fs tunable pulses in Cr:LiSAF. Opt Lett 17:195–197.

Mocker HW, Collins RJ. (1965). Mode competition and self-locking effects in a Q-switched ruby laser. Appl Phys Lett 7:270–273.

Morgner U, Kärtner FX, Cho SH, Chen Y, Haus HA, Fujimoto JG, Ippen EP, Scheuer V, Angelow G, Tschudi T. (1999a). Sub-two-cycle pulses from a Kerr-lens mode-locked Ti:sapphire laser: addenda. Opt Lett 24:920.

Morgner U, Kärtner FX, Cho SH, Chen Y, Haus HA, Fujimoto JG, Ippen EP, Scheuer V, Angelow G, Tschudi T. (1999b). Sub-two-cycle pulses from a Kerr-lens mode-locked Ti:sapphire laser. Opt Lett 24:411–413.

Moulton PF. (1986). Spectroscopic and laser characteristics of Ti:Al_2O_3. J Opt Soc Am B 3:125–132.

Nisoli M, Stagira S, Silvestri SD, Svelto O, Sartania S, Cheng Z, Lenzner M, Spielmann C, Krausz F. (1997). A novel high-energy pulse compression system: generation of multigigawatt sub-5-fs pulses. Appl Phys B 65:189–196.

Page RH, Schaffers KI, DeLoach LD, Wilke GD, Patel FD, Tassano JB, Payne SA, Krupke WF, Chen K-T, Burger A. (1997). Cr^{2+}-doped zinc chalcogenides as efficient, widely tunable mid-infrared lasers. IEEE J Quantum Electron 33:609–619.

Paschotta R, Aus der Au J, Keller U. (1999a). Strongly enhanced negative dispersion from thermal lensing or other focussing elements in femtosecond laser cavities. J Opt Soc Am B 17:646–651.

Paschotta R, Aus der Au J, Keller U. (2000b). Thermal effects in high power end-pumped lasers with elliptical mode geometry. J Selected Topics Quantum Electron 6:636–642.

Paschotta R, Aus der Au J, Spühler GJ, Morier-Genoud F, Hövel R, Moser M, Erhard S, Karszewski M, Giesen A, Keller U. (2000a). Diode-pumped passively mode-locked lasers with high average power. Appl Phys B 70:S25–S31.

Paschotta R, Spühler GJ, Sutter DH, Matuschek N, Keller U, Moser M, Hövel R, Scheuer V, Angelow G, Tschudi T. (1999b). Double-chirped semiconductor mirror for dispersion compensation in femtosecond lasers. Appl Phys Lett 75:2166–2168.

Petrov V, Shcheslavskiy V, Mirtchev T, Noack F, Itatani T, Sugaya T, Nakagawa T. (1998). High-power self-starting femtosecond Cr:forsterite laser. Electron Lett 34:559–561.

Ramaswamy M, Gouveia-Neto AS, Negus DK, Izatt JA, Fujimoto JG. (1993). 2.3-ps pulses from a Kerr-lens mode-locked lamp-pumped Nd: YLF laser with a microdot mirror. Opt Lett 18:1825–1827.

Ramaswamy-Paye M, Fujimoto JG. (1994). Compact dispersion-compensating geometry for Kerr-lens mode-locked femtosecond lasers. Opt Lett 19:1756–1758.

Roskos H, Robl T, Seilmeier A. (1986). Pulse shortening to 25 ps in a cw mode-locked Nd:YAG laser by introducing an intracavity etalon. Appl Phys B 40:59–65.

Rothenberg JE. (1992). Space-time focusing: breakdown of slowly varying envelope approximation in the self-focusing of femtosecond pulses. Opt Lett 17:1340–1342.

Ruddock IS, Bradley DJ. (1976). Bandwidth-limited subpicosecond pulse generation in modelocked cw dye lasers. Appl Phys Lett 29:296–297.

Ruffing B, Nebel A, Wallenstein R. (1997). A 20-W KTA-OPO synchronously pumped by a cw modelocked Nd:YVO_4 oscillator-amplifier system, Conference on Lasers and Electro-Optics. OSA Tech Dig Ser Vol II, CWB2. New York: Opt Soc Am: p 199.

Sarukura N, Ishida Y, Nakano H. (1991). Generation of 50 fs pulses from a pulse compressed, cw, passively modelocked Ti:sapphire laser. Opt Lett 16:153–155.

Sennaroglu A, Pollock CR, Nathel H. (1993). Generation of 48-fs pulses and measurement of crystal dispersion by using a regeneratively initiated self-mode-locked chromium-doped forsterite laser. Opt Lett 18:826–828.

Sennaroglu A, Pollock CR, Nathel H. (1994). Continuous-wave self-modelocked operation of a femtosecond Cr^{4+}:YAG laser. Opt Lett 19:390–392.

Shank CV, Ippen EP. (1974). Subpicosecond kilowatt pulses from a modelocked cw dye laser. Appl Phys Lett 24:373–375.

Shirakawa A, Sakane I, Takasaka M, Kobayashi T. (1999). Sub-5-fs visible pulse generation by pulse-front-matched noncollinear optical parametric amplification. Appl Phys Lett 74:2268–2270.

Sorokina IT, Sorokin E, Wintner E, Cassanho A, Jenssen HP, Szipöcs R. (1997). 14-fs pulse generation in Kerr-lens modelocked prismless Cr:LiSGaF and Cr:LiSAF lasers: observation of pulse self-frequency shift. Opt Lett 22:1716–1718.

Spence DE, Kean PN, Sibbett W. (1991). 60-fsec pulse generation from a self-modelocked Ti:sapphire laser. Opt Lett 16:42–44.

Spielmann C, Krausz F, Brabec T, Wintner E, Schmidt AJ. (1991). Femtosecond passive modelocking of a solid-state laser by dispersively balanced nonlinear interferometer. Appl Phys Lett 58:2470–2472.

Spühler GJ, Paschotta R, Kullberg MP, Graf M, Moser M, Mix E, Huber G, Harder C, Keller U. (2001). A passively Q-switched Yb:YAG microchip laser. Appl Phys B 72:285–287.

Spühler GJ, Südmeyer T, Paschotta R, Moser M, Weingarten KJ, Keller U. (2000). Passively mode-locked high-power Nd:YAG lasers with multiple laser heads. Appl Phys B 71:19–25.

Steinmeyer G, Sutter DH, Gallmann L, Matuschek N, Keller U. (1999). Frontiers in ultrasoft pulse generation: pushing the limits in linear and nonlinear optics. Science 286:1507–1512.

Sutter DH, Gallmann L, Matuschek N, Morier-Genoud F, Scheuer V, Angelow G, Tschudi T, Steinmeyer G, Keller U. (2000). Sub-6-fs pulses from a SESAM-assisted Kerr-lens modelocked Ti:sapphire laser: at the frontiers of ultrashort pulse generation. Appl Phys B 70:S5–S12.

Sutter DH, Steinmeyer G, Gallmann L, Matuschek N, Morier-Genoud F, Keller U, Scheuer V, Angelow G, Tschudi T. (1999). Semiconductor saturable-absorber mirror-assisted Kerr-lens mode-locked Ti:sapphire laser producing pulses in the two-cycle regime. Opt Lett 24:631–633.

Tomaru T, Petek H. (2000). Femtosecond Cr^{4+}:YAG laser with an L-fold cavity operating at a 1.2 GHz repetition rate. Opt Lett 25:584–586.

Tong YP, French PMW, Taylor JR, Fujimoto JO. (1997). All-solid-state femtosecond sources in the near infrared. Opt Commun 136:235–238.

Tsuda S, Knox WH, De Souza EA, Jan WY, Cunningham JE. (1995). Low-loss intracavity AlAs/AlGaAs saturable Bragg reflector for femtosecond mode locking in solid-state lasers. Opt Lett 20:1406–1408.

Uemura S, Torizuka K. (1999). Generation of 12-fs pulses from a diode-pumped Kerr-lens mode-locked Cr:LiSAF laser. Opt Lett 24:780–782.

Valdmanis JA, Fork RL, Gordon JP. (1985). Generation of optical pulses as short as 27 fs directly from a laser balancing self-phase moduation, group-velocity dispersion, saturable absorption, and saturable gain. Opt Lett 10:131–133.

Valentine GJ, Kemp AJ, Birkin DJL, Burns D, Balembois F, Georges P, Bernas H, Aron A, Aka G, Sibbett W, Brun A, Dawson MD, Bente E. (2000). Femtosecond Yb:YCOB laser pumped by narrow-stripe laser diode and passively modelocked using ion implanted saturable-absorber mirror. Electron Lett 36:1621–1623.

Walker SJ, Avramopoulos H, Sizer T. (1990). Compact mode-locked solid-state lasers at 0.5- and 1-GHz repetition rates. Opt Lett 15:1070–1072.

Walker AC, Kar AK, Ji W, Keller U, Smith SD. (1986). All-optical power limiting of CO_2 laser pulses using cascaded optical bistable elements. Appl Phys Lett 48:683–685.

Wang HS, LikamWa P, Lefaucheur JL, Chai BHT, Miller A. (1994). Cw and self-mode-locking performance of a red pumped Cr:LiSCAF laser. Opt Commun 110:679–688.

Weingarten KJ, Godil AA, Gifford M. (1992). FM modelocking at 2.85 GHz using a microwave resonant optical modulator. IEEE Photon Technol Lett 4:1106–1109.

Weingarten KJ, Keller U, Chiu TH, Ferguson JF. (1993). Passively mode-locked diode-pumped solid-state lasers that use an antiresonant Fabry-Perot saturable absorber. Opt Lett 18:640–642.

Weingarten KJ, Shannon DC, Wallace RW, Keller U. (1990). Two gigahertz repetition rate, diode-pumped, mode-locked, Nd:yttrium lithium fluoride (YLF) laser. Opt Lett 15:962–964.

Xu L, Tempea G, Spielmann C, Krausz F. (1998). Continuous-wave mode-locked Ti:sapphire laser focusable to $5 \times 10^{13}\,W/cm^2$. Opt Lett 23:789–791.

Yakymyshyn P, Pinto JF, Pollock CR. (1989). Additive pulse modelocked NaCl:OH-laser. Opt Lett 14:621–623.

Yan L, Ling JD, Ho P-T, Lee CH. (1986). Picosecond-pulse generation from a continuous-wave neodymium: phosphate glass laser. Opt Lett 11:502–503.

Yanovsky VP, Wise FW, Cassanho A, Jenssen HP. (1995). Kerr-lens mode-locked diode-pumped Cr:LiSGAF laser. Opt Lett 20:1304–1306.

Zhang Z, Nakagawa T, Torizuka K, Sugaya T, Kobayashi K. (1999). Self-starting modelocked Cr^{4+}:YAG laser with a low-loss broadband semiconductor saturable-absorber mirror. Opt Lett 24:1768–1770.

Zhang Z, Torizuka K, Itatani T, Kobayashi K, Sugaya T, Nakagawa T. (1997a). Self-starting mode-locked femtosecond forsterite laser with a semiconductor saturable-absorber mirror. Opt Lett 22:1006–1008.

Zhang Z, Torizuka K, Itatani T, Kobayashi K, Sugaya T, Nakagawa T. (1997b). Femtosecond Cr:forsterite laser with modelocking initiated by a quantum well saturable absorber. IEEE J Quantum Electron 33:1975–1981.

Zhou F, Malcolm GPA, Ferguson AI. (1991). 1-GHz repetition-rate frequency-modulation mode-locked neodymium lasers at 1.3 μm. Opt Lett 16:1101–1103.